

Design, FEM Modeling and Optimization of MEMS based  
Wideband Vibrational Energy Harvester for Low Power  
Applications



*Author*

HASSAN ARSLAN

NUST201464533MCEME35514F

*Supervisor*

Dr. MUHAMMAD MUBASHER SALEEM

Department of Mechatronics Engineering  
College of Electrical & Mechanical Engineering  
National University of Sciences and Technology,  
Islamabad

Design, FEM Modeling and Optimization of MEMS based Wideband  
Vibrational Energy Harvester for Low Power Applications

Author

HASSAN ARSLAN

NUST201464533MCEME35514F

A thesis submitted in partial fulfillment of the requirements for the degree of  
MS Mechatronics Engineering

Thesis Supervisor:

Dr. MUHAMMAD MUBASHER SALEEM

Thesis Supervisor's Signature: \_\_\_\_\_

DEPARTMENT OF MECHATRONICS ENGINEERING  
COLLEGE OF ELECTRICAL & MECHANICAL ENGINEERING  
NATIONAL UNIVERSITY OF SCIENCES AND TECHNOLOGY,  
ISLAMABAD  
MARCH, 2018

## **Declaration**

I certify that this research work titled “*Design, FEM Modeling and Optimization of MEMS based Wideband Vibrational Energy Harvester for Low Power Applications*” is my own work. The work has not been presented elsewhere for assessment. The material that has been used from other sources it has been properly acknowledged / referred.

Signature of Student

Hassan Arslan

NUST201464533MCEME35514F

## **Language Correctness Certificate**

This thesis has been read by an English expert and is free of typing, syntax, semantic, grammatical and spelling mistakes. Thesis is also according to the format given by the university.

Signature of Student

Hassan Arslan

NUST201464533MCEME35514F

Signature of Supervisor

## **Copyright Statement**

- Copyright in text of this thesis rests with the student author. Copies (by any process) either in full, or of extracts, may be made online accordance with instructions given by the author and lodged in the Library of NUST College of E&ME. Details may be obtained by the Librarian. This page must form part of any such copies made. Further copies (by any process) may not be made without the permission (in writing) of the author.
- The ownership of any intellectual property rights which may be described in this thesis is vested in NUST College of E&ME, subject to any prior agreement to the contrary, and may not be made available for use by third parties without the written permission of the College of E&ME, which will prescribe the terms and conditions of any such agreement.
- Further information on the conditions under which disclosures and exploitation may take place is available from the Library of NUST College of E&ME, Rawalpindi.

## **Acknowledgements**

I am thankful to my Creator Allah Subhana-Watala to have guided me throughout this work at every step and for every new thought which He setup in my mind to improve it. Indeed I could have done nothing without His priceless help and guidance. Whosoever helped me throughout the course of my thesis, whether my parents or any other individual was His will, so indeed none be worthy of praise but Him.

I am profusely thankful to my beloved parents who raised me when I was not capable of walking and continued to support me throughout in every department of my life.

I am profusely thankful to my supervisor Dr. Muhammad Mubahser Saleem for his counsel throughout my project and for his guidance and cooperation. This work would not have been possible if it were not for my supervisor who kept me pushing hard and gave me his valuable time, knowledge, expertise and attention. I would like to thank all faculty members of department for teaching me useful courses which helped me a lot during my research phase. I would also like to show my gratitude towards Dr. Umar Shahbaz Khan, Head DMTS for administrative support.

I would like to acknowledge the outstanding support provided by my wife, who has rendered valuable assistance, courage and motivations for my study. Finally, I am grateful to my siblings and righteous friends; Asma Asif, Fatima Jamil, and Hafsa Asif.

*Dedicated to my parents for their support and prayers, to my wife for her pronounced motivation and guidance and to my sisters for their love and care*

## Abstract

This thesis presents the design, model and finite element analysis for Electrostatic Vibration Energy Harvester (EVEH). Due to the advancement in the CMOS technology the power ratings for microelectronics are becoming increasingly low due to their reduced size and supplying power to remote microsystems is becoming challenging. A device is needed which can harvest the ambient forms of energy from the surrounding to electrical energy or to make the devices self-powered in order to get rid of batteries. From the beginning of 21st century research efforts were made to find the mechanisms to harvest these ambient forms of energies. Usually three main transduction mechanisms for vibration based energy harvesters exist which are piezoelectric, electrostatic and electromagnetic, among these techniques electrostatic energy harvester is considered better due to its ease of integration with microelectronics. The novelty of the proposed harvester in this thesis is that it utilizes three degrees of freedom with amplification in displacement of proof mass and designed in a way that maximum number of transduction units (comb drives) are attached with absorber masses. A low cost commercially available fabrication process Metal MUMPs provided by MEMSCAP is selected. Usually three types of processes are provided by MEMSCAP those are SOIMUMPs, PolyMUMPs and MetalMUMPs, all differs with each other in a material usage for structural layer and minimum feature size. This MetalMUMPs process has minimum feature size of  $8 \mu m$  and thickness of  $20 \mu m$  with a structural layer of nickel. The resonance frequency of the harvester is around 3.9 kHz and very low acceleration amplitude of 0.1 g. The area of the proposed device is  $7.48 mm^2$  and overlapping length of the combs attached is  $25 \mu m$ . The total mass of the device is 9.4 mg with device volume of  $0.140 mm^3$  having normalized power density of  $0.0032 mW/cm^3 g^{-2}$ . The total harvested power for applied load of 0.1 g was calculated to be 4.2 nW.

# Table of Contents

<b>Declaration .....</b>	<b>i</b>
<b>Language Correctness Certificate.....</b>	<b>ii</b>
<b>Copyright Statement .....</b>	<b>iii</b>
<b>Acknowledgements .....</b>	<b>iv</b>
<b>Abstract .....</b>	<b>vi</b>
<b>Table of Contents.....</b>	<b>vii</b>
<b>List of Figures .....</b>	<b>ix</b>
<b>List of Tables.....</b>	<b>x</b>
<b>CHAPTER 1: INTRODUCTION.....</b>	<b>1</b>
1.1 Overview.....	1
1.2 Sources of energy harvesting .....	1
1.2.1 Solar energy .....	2
1.2.2 Thermal energy .....	2
1.3 Vibration energy .....	2
1.3.1 Transduction techniques .....	4
1.3.2 Piezoelectric energy harvester .....	4
1.3.3 Electrostatic energy harvester .....	5
1.3.4 Electromagnetic harvester.....	5
1.4 Literature review .....	6
1.5 Categories of EVEH.....	12
1.5.1 In-plane Gap Closing .....	12
1.5.2 In-plane Overlap .....	13
1.5.3 Out of plane Gap Varying Converter .....	14
1.5.4 In-Plane with Variable Surface.....	15
1.6 EVEH working principle.....	15
1.7 Scavenging mechanisms .....	16
1.7.1 Charge-constrained cycle.....	16
1.7.2 Voltage-constrained cycle.....	17
1.8 Challenges in EEHs.....	18
1.9 Problem formulation .....	19
1.10 Thesis outline .....	20
<b>CHAPTER 2: 3-DOF ELECTROSTATIC ENERGY HARVESTER.....</b>	<b>21</b>
2.1 Concept of resonators.....	21
2.2 Proposed 3-DOF system .....	25
2.3 Equations of 3-DOF system .....	26
2.4 Calculation of natural frequencies by Eigen-value method.....	28

2.5	Advantage of In-plane-overlap design .....	29
<b>CHAPTER 3: DESIGN AND ANALYTICAL SIMULATIONS OF THE PROPOSED DESIGN .....</b>		<b>30</b>
3.1	Overview .....	30
3.2	Proposed design .....	30
3.3	Mechanical design elements of proposed device .....	32
3.3.1	Suspension design .....	33
3.3.2	Damping .....	35
3.4	Design parameters of proposed device .....	37
<b>CHAPTER 4: FINITE ELEMENT ANALYSIS .....</b>		<b>39</b>
4.1	Overview .....	39
4.2	Design specifications .....	39
4.3	FEM Analysis .....	39
4.3.1	Material properties .....	40
4.3.2	Optimization .....	40
4.3.3	Modal analysis in ANSYS and COMSOL .....	41
4.3.4	Harmonic analysis in ANSYS and COMSOL .....	44
4.4	Output Power .....	50
4.5	Power Density .....	51
4.6	Comparison with Previous Work .....	51
<b>CHAPTER 5: CONCLUSION AND FUTURE PROSPECTS .....</b>		<b>52</b>
5.1	Conclusion .....	52
5.2	Future Work and Recommendations .....	52
<b>REFERENCES .....</b>		<b>54</b>

## List of Figures

<b>Figure 1-1</b> Electrostatic converter with charge electrodes [20] .....	5
<b>Figure 1-2</b> Electromagnetic conversion device by Amirtharajah and Chandrakasan, 1988 [23]. .	6
<b>Figure 1-3</b> Proposed deign of Menninger et al [27].....	7
<b>Figure 1-4</b> Multi-Degree of freedom Energy harvester [29].....	8
<b>Figure 1-5</b> Microscopic view of energy harvester [30].....	8
<b>Figure 1-6</b> Despesse et al device design [31].....	9
<b>Figure 1-7</b> Schematic of single cantilever device [32] .....	9
<b>Figure 1-8</b> Schematic of device proposed by Tao [33].....	10
<b>Figure 1-9</b> Schematic of In-plane-gap-closing topology [20].....	13
<b>Figure 1-10</b> Schematic of In-plane-overlap topology [20] .....	14
<b>Figure 1-11</b> Schematic of Out-of-plane gap varying topology [20] .....	14
<b>Figure 1-12</b> Schematic of In-plane with variable surface topology [20] .....	15
<b>Figure 1-13</b> Energy scavenging cycles [1].....	16
<b>Figure 1-14</b> Charge-constrained cycle for EEHs [1] .....	17
<b>Figure 1-15</b> Voltage-constrained cycle for EEHs [1] .....	18
<b>Figure 2-1</b> schematic of resonator by Dyck [55] .....	21
<b>Figure 2-2</b> Frequency Response of dual mass oscillator [56].....	22
<b>Figure 2-3</b> schematic of resonator by Sahin (2009) [55] .....	23
<b>Figure 2-4</b> Coupled resonator (3-DOF) concept by Erismis [55] .....	23
<b>Figure 2-5</b> Frequency Response of 3-DOF resonator [55] .....	24
<b>Figure 2-6</b> Proposed schematic for 3-DOF system [55] .....	26
<b>Figure 2-7</b> Frequency response of un-damped system.....	28
<b>Figure 3-1</b> Design of Proposed device.....	31
<b>Figure 3-2</b> Different suspension designs [61].....	33
<b>Figure 3-3</b> Folded flexure used in proposed device.....	34
<b>Figure 4-1</b> meshed design in COMSOL 5.2 .....	39
<b>Figure 4-2</b> Un-damped frequency response in Matlab for the proposed design.....	40
<b>Figure 4-3</b> Damped frequency response in Matlab for the proposed design .....	40
<b>Figure 4-4</b> Second mode shape in COMSOL .....	44
<b>Figure 4-5</b> phase response of un-damped system in Matlab.....	45
<b>Figure 4-6</b> phase response of damped system in COMSOL 5.2.....	45
<b>Figure 4-7</b> Frequency response graph in COMSOL .....	49
<b>Figure 4-8</b> Frequency response graph in ANSYS.....	49
<b>Figure 4-9</b> Comb-drives attached with absorber mass.....	50
<b>Figure 5-1</b> Block diagram for power management circuitry [20].....	53

## List of Tables

<b>Table 1-1</b> Energy harvesting techniques with power densities and source.....	1
<b>Table 1-2</b> List of vibration sources with peak acceleration and frequency of operation .....	3
<b>Table 1-3</b> Literature survey comparison .....	11
<b>Table 1-4</b> Different electret materials .....	11
<b>Table 2-1</b> Natural frequencies of proposed system.....	29
<b>Table 3-1</b> Design parameters of the proposed device .....	37
<b>Table 4-1</b> first six modes of natural frequencies .....	41
<b>Table 4-2</b> Different mode shapes explained.....	42
<b>Table 4-3</b> displacement profiles of the device in COMSOL.....	47

# CHAPTER 1: INTRODUCTION

## 1.1 Overview

The different techniques used to scavenge, capture or harvest unused ambient form of energy (e.g., wind, thermal, solar and vibration) which exist in the surrounding environment in our daily life, and convert that captured energy in to electrical energy to operate low-power electronic devices or to recharge batteries is called energy harvesting or energy scavenging [1, 2]. Batteries have been the primary source of power used for low-power applications, but due to their limited life-time and difficulty of replacement in some uses such as implanted biomedical devices and wireless sensors, they are not the center of attention anymore. These problems needed an appealing solution and a self-powered system, which is energy harvesting from ambient sources [3, 4].

As advancement in CMOS VLSI technology enabled us to build low-power microelectronic devices, these devices should be made independent in energy requirements. These devices will generate their power by themselves using different transduction mechanisms such as solar, thermal, wind and mechanical vibrations.

## 1.2 Sources of energy harvesting

An extensive survey of energy harvesting techniques has been attempted. The outcomes of this survey are listed in Table 1-1. The values given in the Table are gathered from different published work in the field of energy harvesting.

**Table 1-1** Energy harvesting techniques with power densities and source

<b>Energy Harvester Technique</b>	<b>Power Density (<math>\mu\text{W}/\text{cm}^3</math>) 1 year life time</b>	<b>Power Density (<math>\mu\text{W}/\text{cm}^3</math>) 10 year life time</b>	<b>Source</b>
Solar (Outdoors)	15,000 – direct sun 150 – cloudy day	15,000 – direct sun 150 – cloudy day	[5]
Solar (Indoors)	6 – office desk	6 – office desk	-
Vibrations	200	200	[6]

Acoustic Noise	0.003 @ 75 Db 0.96 @ 100 Db	0.003 @ 75 Db 0.96 @ 100 Db	[5]
Temperature Gradient	15 @ 10oC gradient	15 @ 10oC gradient	[3]

### 1.2.1 Solar energy

The solar power defined as the output from solar cells when sunlight strikes it causing current to flow in the cell. Power from solar radiation is the most abundant source of energy. During a typical bright sunny day the power density provided by the solar cell is first-rate but it drops down drastically in dim light or cloudy weather and hence solar energy is not a complete solution for embedded systems as no light is existent in most of the cases for such type of systems.

During daytime energy from the solar cell show a power density of about 100mW per square centimeter which is quite good and sufficient to operate microelectronic devices or micro-sensors. If the desired application is to be operated outdoors only in the day time then solar cell is a mature solution. Therefore solar cells have very limited applications because of the cited shortcomings [7].

### 1.2.2 Thermal energy

Electrical power generated by temperature differences, gradients, and from heat is known to be thermal energy harvesting. Thermal transducers utilize See-beck effect to convert thermal energy in to electrical energy [8]. The phenomena in which two different electrical conductors having a variance in their temperatures result in a voltage difference between the two conductors. Usually the order of few nano watts power can be generated by these type of transducers.

### 1.3 Vibration energy

Vibrations are defined as the mechanical phenomena of oscillations or to and fro motion about an equilibrium point. Vibrations are present everywhere in our daily life e.g. motion of suspended bridge under different stresses, car engine vibrations, base of machines in heavy

industries, washing machines, refrigerators etc. Vibration energy is wasted in most of the cases in which oscillations are undesirable so in order to harvest that surplus energy in to useful electrical energy, different transduction techniques are used which includes using piezoelectric, electrostatic or electromagnetic mechanisms. The objective of this thesis is to harvest vibration energy in to electrical energy using electrostatic technique. As vibrations to electrical conversion are not possible in all environments so specific sources of vibrations are considered with their maximum acceleration magnitude and ranges of frequency where maximum amplitude of vibrations arises [5, 9-11]. A list of sources with acceleration amplitude and frequencies are listed in Table 1-2 [12].

**Table 1-2** List of vibration sources with peak acceleration and frequency of operation

<b>Sources of vibration</b>	<b>Peak Acceleration (ms<sup>-2</sup>)</b>	<b>Frequency of peak amplitude (Hz)</b>
Car engine	12	200
Base of 3 axis machine tool	10	70
Blender casing	6.4	121
Clothes dryer	3.5	121
Door frame just after door closes	3	125
Small microwave oven	2.25	121
HVAC vents in office building	0.2 - 1.5	60
Wooden deck with people walking	1.3	385
Bread maker	1.03	121
Notebook computer while CD is being read	0.6	75
Washing machine	0.5	109
Second story floor of office	0.2	100
Refrigerator	0.1	240

### **1.3.1 Transduction techniques**

In order to generate electrical energy from vibrations the mechanisms are required to convert one form of energy into other useful form. Some of the vibration harvesters utilize strains or pressure and mechanically deform to convert mechanical energy in to electrical energy such as piezoelectric harvesters. Others use the relative motion coupled with transduction mechanism as in the case of electromagnetic and electrostatic generators. Each technique has advantages and disadvantages regarding size of the device and output power along with frequency bandwidth region of oscillating energy harvester [13].

Typically three transduction mechanisms are used to convert mechanical oscillatory- motion in to electrical energy. These techniques are: piezoelectric, electrostatic and electromagnetic.

### **1.3.2 Piezoelectric energy harvester**

Piezoelectric generators convert ambient vibrations in to electrical power by utilizing their material based property of generating electric charge in the response of mechanical stress [14-16]. When pressure is applied on these crystals, the deformation in their shape results in the formation of electric charges because external mechanical force rearranges the dipoles present in the crystal. This rearrangement leads to change in the dipole density which changes the electric field between dipoles. Therefore, change in electric field produces an electric power. Piezoelectric generators have certain advantages and disadvantages at micro scale energy harvesting. The piezoelectric harvesters generate voltages without using external power source or bias voltage. Another advantage is that mechanical stoppers are not required in order to control the relative displacement and in fact output power produced is enough for micro level devices to operate independently. The major disadvantage of piezoelectric harvesters is complexity of integration with microelectronic circuitry.

### 1.3.3 Electrostatic energy harvester

Electrostatic vibration energy harvester can generate electrical power by the relative motion between the two conductors while both conductors are charged so that relative movement against the electrostatic force yields in electrical power [17-19]. The capacitive mechanism is shown in Figure 1.1

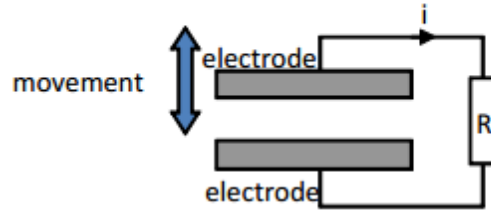


**Figure 1-1** Electrostatic converter with charge electrodes [20]

The major advantage of electrostatic vibration energy harvester is their compatibility with microelectronic devices which makes them very suitable as an independent power source. Electrostatic and electromagnetic dynamic energy harvesters do not require costly and smart materials like piezoelectric and magneto restrictive. Electrostatic types are economical to fabricate. The disadvantage of these types of generators is that they need mechanical stoppers to control the vibration amplitude which results in high mechanical damping and the requirement of extra voltage source to initially charge the plates which affects the performance and shows dependency on external voltage sources.

### 1.3.4 Electromagnetic harvester

The electromagnetic vibration energy harvester utilizes the motion of coil (inductor) with in magnetic field produced by permanent magnet [9, 21, 22]. This movement of coil with in magnetic field results in current flow (induced EMF) in the coil. A device with such characteristics is shown below in Figure 1-2.

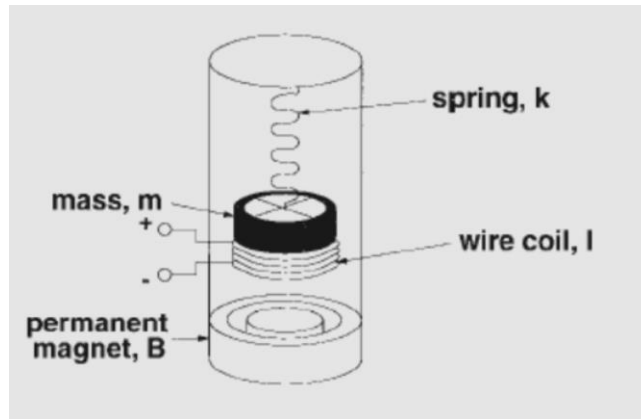


**Figure 1-2** Electromagnetic conversion device by Amirtharajah and Chandrakasan, 1988 [23].

The output power obtained from electromagnetic vibration energy harvester is in the orders of several mW which is good enough for micro devices.

## 1.4 Literature review

Electrostatic energy harvesters (EEHs) has several advantages including its easy fabrication, suitability for low frequency applications, integration with microelectronic systems, and higher output voltages (2-10) volts. The fabrication process in these EEHs is compatible with processing techniques of microelectromechanical systems (MEMS). Moreover, power density of EEHs is increased by reduction in size. However, the major drawback associated with EEHs is the requisite of an external voltage source and during operation accurate conversion circuit is required in order to extract the electrical energy from vibrational sources [13, 24] . EEHs have structure similar to capacitors with two conductive plates separated by dielectric medium. The electrical energy is generated by relative motion of these two conductive plates which generates a variation in capacitance. The EEHs are further divided into two types;

- Electret-free EEHs
- Electret-based EEHs

The advancement in IC technologies deems it possible for micro devices to operate at low power such as wireless sensor nodes. These can be operated at less than 1 mW [25]. The wireless sensor nodes are used for measuring humidity, pressure variations or air flow, speed in an environment, or in an industry for monitoring purposes. In order to operate these devices using batteries is not

the feasible solution, therefore MEMS based harvesters are designed to provide power to these devices indefinitely.

Kuehne et al.[26] designed a vibrational electrostatic energy harvester utilizing out-of-plane gap closing topology which provided  $4.28\mu\text{W}$  with acceleration of  $0.2\text{g}$  at  $1\text{ KHz}$ .

Meninger et al.[27] have proposed vibration based electrostatic harvester having an area of  $1.5\text{ cm}^2 - 0.5\text{ cm}^2$  with thickness of  $500\ \mu\text{m}$ . The output power at resonance frequency of  $2520\text{ Hz}$  was  $8\mu\text{W}$  and power density of the device was  $0.11\mu\text{W}/\text{mm}^3$ .

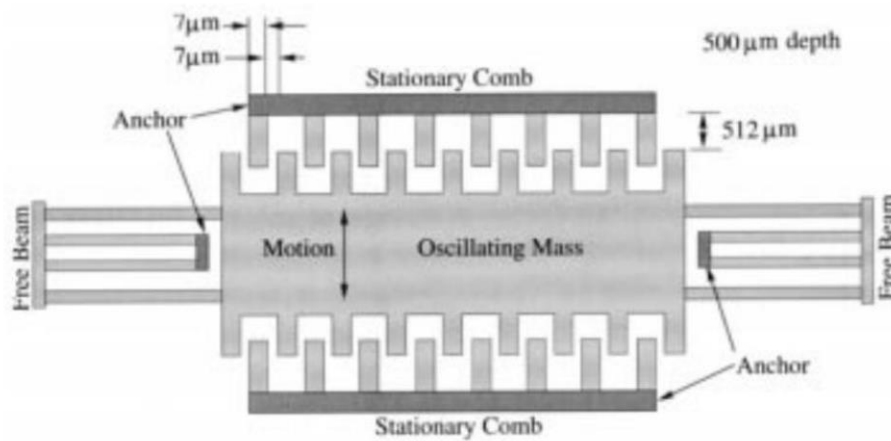


**Figure 1-3** Proposed design of Meninger et al [27]

Chiu et al.[28] have designed a device using in-plane gap closing mechanism to harvest  $1.2\mu\text{W}$  with  $5\text{ M}\Omega$  load at  $1.8\text{ KHz}$  having  $1\text{ cm}^2$  device area.

Zijing Wong et al.[29] have developed a multi degree of freedom electrostatic MEMS based power generator to harvest multiple frequencies. The multi-frequency design was able to harvest more power from different values of vibration frequencies. It generated  $0.076\ \mu\text{W}$  at  $1.4\text{ KHz}$  with acceleration amplitude of  $2.5\text{ g}$ .

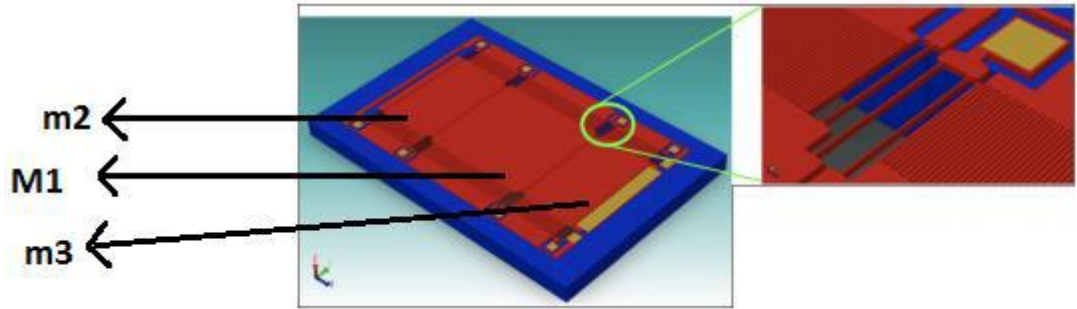


**Figure 1-4** Multi-Degree of freedom Energy harvester [29]

Daniel Hoffmann et al [30] developed a harvester, shown in Figure 1-5, with size of 5 mm X 6 mm which produced 3.5  $\mu$ W at vibration amplitude of 13 g with 1.3-1.5 KHz frequency.

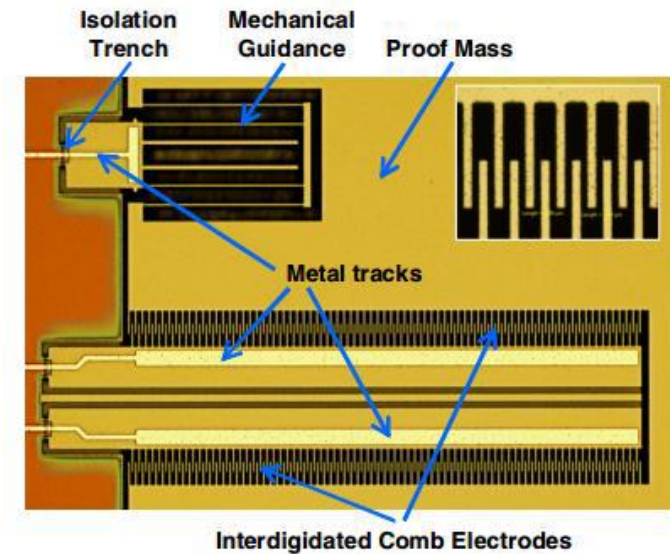


**Figure 1-5** Microscopic view of energy harvester [30]

Despesse et al [31] presented electrostatic vibration energy harvester having a large mass, shown in Figure 1-6. The structural layer of the harvester was made of bulk tungsten. Due to the very large volume of the device, resonance frequency of the device came at 50 Hz and output power of 1052  $\mu$ W was scavenged. The device used in plane gap closing type topology.

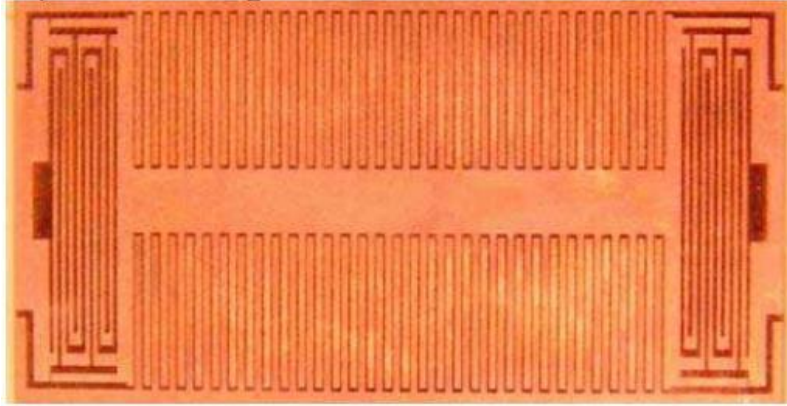


**Figure 1-6** Despesse et al device design [31]

Zhang *et al* [32] in 2016 presented a device with single cantilever consisting of proof mass attached at one end, Figure 1-7. The device utilizes electrostatic effect to harvest energy from random vibrations in the range of 36.3 – 48.3 Hz. Output power at 1 g external acceleration was about 6.2 – 9.8  $\mu$ W.

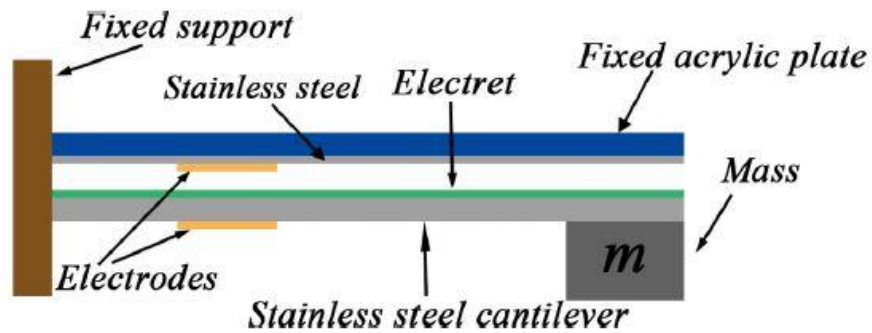


**Figure 1-7** Schematic of single cantilever device [32]

Tao *et al* [33] proposed an electret based device consisting of sandwiched electrode layer between two oppositely charged electret layers. The resonant frequency of the device, Figure 1-8, was calculated through finite element analysis was 147 Hz. Output voltage of 4.8 V was achieved experimentally at 120 Hz at 15  $\text{ms}^{-2}$  input acceleration.

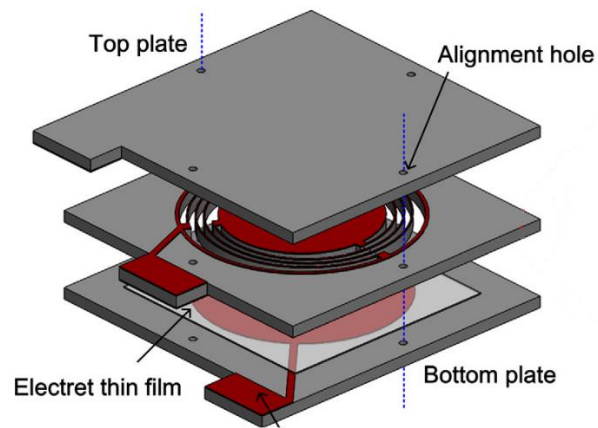


**Figure 1-8** Schematic of device proposed by Tao [33]

The device is pretty complicated to be designed due to two layers of electret with opposite charges. The charging process for both layers is different and the gap between the plates has to be precise in order for the charged layers to take effect on electrode layer. Despite all these complications, the output voltage was increased by 80% as compared to single electret layer devices.

The Electret free EEHs are normally considered as passive device. The transformation of mechanical energy into electrical energy is usually achieved by energy cycles including, charge constrained and voltage constrained cycles. A detailed comparison of previous research is compiled into Table 1-3.

However, the electret based EEHs have additional electret layers that are added on conductive plates (either one or both) of variable capacitive device. The operation of electret based EEHs are similar to electret based EEHs. The electrets on conductive plates are charged before starting the operation that is capable of extracting electrical energy from mechanical vibrations. The word electret is derived from two words electricity (electr) and magnet (et). These electrets are usually dielectric materials with electric charges or have dipole polarization. The few electret materials are listed below in Table 1-4. Among them SiO<sub>2</sub> and SiN<sub>3</sub> have high surface charge density compared to others.

**Table 1-3** Literature survey comparison

Reference	Dimensions (Volume : mm <sup>3</sup> ) (Area : mm <sup>2</sup> )	Frequency (Hz)	Acceleration (g)	Bias Voltage (V)	Power ( $\mu$ W)
Meninger <i>et al</i> [27]	75 mm <sup>3</sup>	2520	-	-	64
Roundy <i>et al</i> [12]	1000 mm <sup>3</sup>	120	0.22	-	110
Miyazaki <i>et al</i> [34]	-	45	0.008	-	0.12
Sterken <i>et al</i> [35]	-	1200	115	-	100
Despesse <i>et al</i> [31]	1800 mm <sup>3</sup>	50	0.89	120	1052
Despesse <i>et al</i> [31]	32.4 mm <sup>3</sup>	50	9.2	-	70
Peano <i>et al</i> [36]	-	911	16.72	-	50
Yen <i>et al</i> [37]	4356 mm <sup>2</sup>	1560	-	6	9.47
Tsutsumino <i>et al</i> [38]	200 mm <sup>2</sup>	20	-	Electret	37.7
Basset P <i>et al</i> [39]	61.49 mm <sup>3</sup>	250	0.25	8	0.061
Hoffman D <i>et al</i> [30]	200 mm <sup>3</sup>	1460	13	50	2.5
Miao P <i>et al</i> [40]	-	10	-	26	24
Choi DH <i>et al</i> [41]	1000 mm <sup>3</sup>	1	-	1	35.3
Basset P <i>et al</i> [42]	42 mm <sup>3</sup>	150	1	30	2.2
Fei Wang <i>et al</i> [19]	1000 mm <sup>2</sup>	98	1	Electret	0.15
Vitaly D <i>et al</i> [43]	48 mm <sup>3</sup>	150	1.5	20	2.2
Zhang <i>et al</i> [32]	-	36-48	1	Electret	6.2-9.8
Tao <i>et al</i> [44]	0.24 cm <sup>3</sup>	100-125	5-15 ms <sup>-2</sup>	Electret	2.8-4.8 V

**Table 1-4** Different electret materials

Materials	Dielectric Constant	Surface charge density	Reference
SiO <sub>2</sub>	3.9	13.5	[45]
SiN <sub>3</sub>	7.5	13.5	[46]
CYTOP™	2.1	1.5	[47]
Teflon	2.1	0.1	[72]

These electrets require initial charging for conversion of mechanical vibrations in electrical energy [38, 48, 49]. For this purpose, after electret fabrication it is subjected to corona charging, which is a process done through corona discharge at very high voltages. A corona discharge is an electrical discharge brought on by the ionization of a fluid such as air surrounding a conductor that is electrically charged at high voltages. This process is used to deposit charge on electrets which can store the charge up to several years depending on the decaying constant, which explains the speed by which the charge on the electret will decay over time.

## **1.5 Categories of EVEH**

MEMS energy harvesters (electrostatic) are usually designed keeping 4 fundamental topologies in mind [20]. These topologies are:

- ❖ In-plane Gap Closing
- ❖ In-plane Overlap
- ❖ Out-of-plane Gap Closing
- ❖ In-Plane with Variable Surface

### **1.5.1 In-plane Gap Closing**

As shown in Figure 1-9 in this type of variable capacitor capacitance changes by changing overlap area within fixed and movable combs. When proof mass is excited by some outer ambient vibrations it will oscillates around it's equilibrium position due to restoring force provided by springs and this change in capacitance results in electrical energy from ambient vibrations.

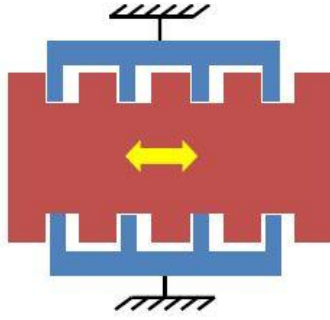


**Figure 1-9** Schematic of In-plane-gap-closing topology [20]

The total capacitance of the IPGC device is given by equation (1-1)

$$C = \frac{2N\epsilon\epsilon_0LH}{g^2-x^2} \quad (1-1)$$

Where,

N = number of electrode fingers

$\epsilon$  = permittivity of dielectric

$\epsilon_0$  = permittivity of free space

L = Length of the electrode fingers

H = height of the electrode fingers

g = initial gap between fingers

x = distance traveled by electrode fingers

### 1.5.2 In-plane Overlap

The capacitance varied by changing the gap between two facing combs. When movable comb moves toward fixed comb the capacitance changes from  $C_{min}$  to  $C_{max}$  so higher the deflection of spring greater is the  $C_{max}$  value. In this converter for single mechanical oscillation two electrical energy cycles are obtained similar to in-plane overlap varying. The design is shown in Figure 1-10.

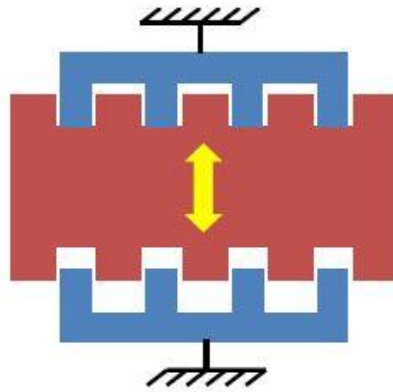


**Figure 1-10** Schematic of In-plane-overlap topology [20]

The total capacitance of the IPO device is given by equation (1-2)

$$C = \frac{2N\epsilon\epsilon_0(L_0+x)}{g} \quad (1-2)$$

### 1.5.3 Out of plane Gap Varying Converter

Out of plane gap closing converter converts mechanical vibrations into electrical energy by changing its capacitance and this can be done by moving the movable electrode plate towards and away from fixed plate. The diagram 1-11 shows the converter.

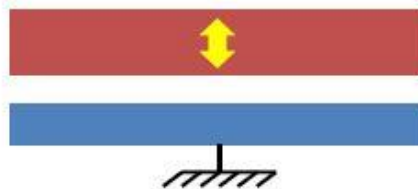


**Figure 1-11** Schematic of Out-of-plane gap varying topology [20]

The total capacitance of the OPGV topology can be calculated using the formula (1-3)

$$C = \frac{N\epsilon\epsilon_0LH}{g-x} \quad (1-3)$$

### 1.5.4 In-Plane with Variable Surface

The in-plane with variable surface topology has capacitance varied by changing the gap between two facing combs. It could be smooth or toothed surface for increasing capacitance, number of electrode increases.

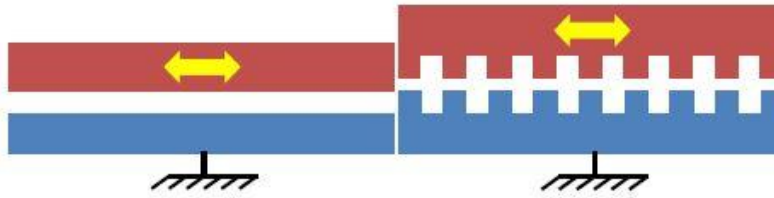


**Figure 1-12** Schematic of In-plane with variable surface topology [20]

Total capacitance is given by equation (1-4)

$$C = \frac{N\epsilon\epsilon_0(L_0-x)}{g} \quad (1-4)$$

### 1.6 EVEH working principle

Variable capacitor is the fundamental block of EVEH comprising following elements

- ❖ central mass,
- ❖ suspensions (springs)
- ❖ dampers
- ❖ comb drives

When the central mass is excited by random vibrations, it starts to oscillate while the suspension provides the restoring force [17, 50, 51]. These oscillations results in capacitance change i.e.  $C_{min}$  to  $C_{max}$  or vice versa as the gap is decreased or increased. This change in capacitance can be converted into useful electrical power by either keeping the voltage constant or the charge, on the electrodes, which is the source of bias. Hence two fundamental conversion cycles for EVEH occurs which are charge constrained and voltage constraint cycle as reported by Menninger et al [27]. In this thesis the charge constrained cycle is used because voltage constrained cycle is more complex.

## 1.7 Scavenging mechanisms

There are two main methods used for harvesting energy from electrostatic devices [20, 40, 52, 53]

### 1.7.1 Charge-constrained cycle

The transformation of mechanical vibrations into electrical energy a charge constrained cycle is illustrated in Figure 1-11. It is very simple to implement cycle in electret free EEHs. In micro machine parallel plates maximum capacitance  $C_{max}$  has been introduced to start the cycle. Initial voltage ( $V_{initial}$ ) which is usually less than maximum voltage is subjected by using an external source. An electric charge  $Q_0$  is stored during the operation on these electret plates. After storage, device is switched to mode of open circuit. The device started to move to the place where it has low capacitance  $C_{min}$  due to presence of vibrations while maintaining electric charge  $Q_0$  as constant. Harvester is connected to load when harvesters reached to maximum voltage and plates are removed by using energy extraction circuit. The total energy is given by

$$E = \frac{1}{2} Q^2 \left( \frac{1}{C_{min}} - \frac{1}{C_{max}} \right) \quad (1-5)$$

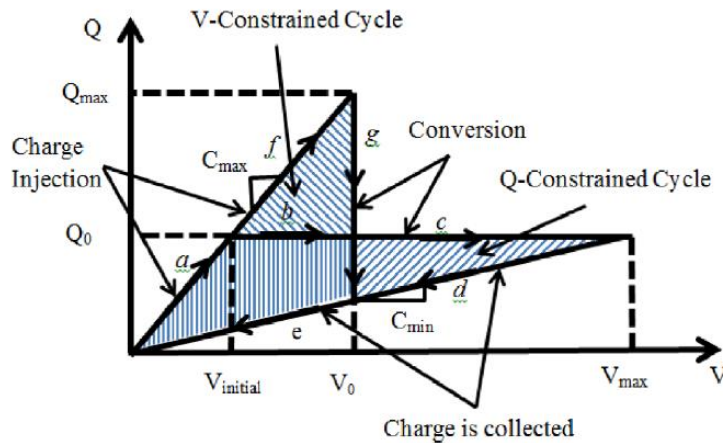


**Figure 1-13** Energy scavenging cycles [1]

Delivered to the external circuit in a charge-constrained cycle is equal to the net area under the curve and can be computed with the stored charge  $Q_0$ , maximum capacitance  $C_{max}$ , and minimum capacitance  $C_{min}$  of the energy harvester's plate during operation.

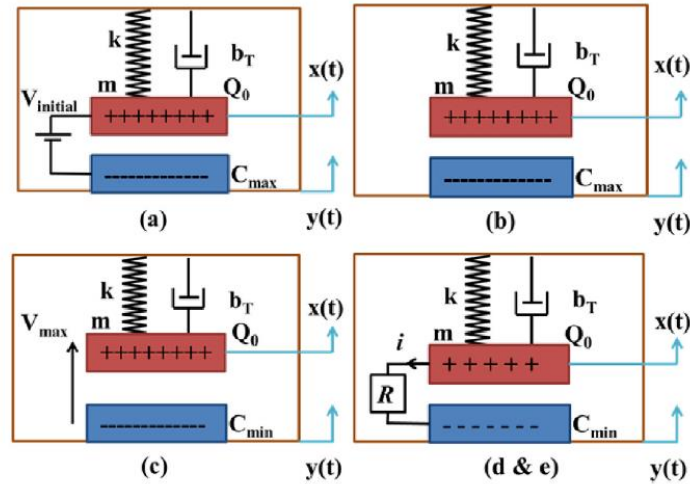


**Figure 1-14** Charge-constrained cycle for EEHs [1]

(a) Charging of EEH at  $C_{max}$ , (b) open circuit mode of EEH, (c) relative movement between the plates to achieve  $C_{min}$ , (d) and (e) discharging of EEH

Figure 1-14 explains the charge constrained cycle in more detail. The capacitor plates, at (a) are charged by a bias voltage  $V_{initial}$ . The charges accumulated on the plates are kept by disconnecting the bias from device. At (c) the displacement in the plates causes the capacitance to change which results in the last phase (d & e) where the plates are discharged and charges flow out of the device powering external circuitry. The next cycle starts when the discharge happens and external bias voltage is re-connected to the plates.

### 1.7.2 Voltage-constrained cycle

Unlike charge constrained cycle, the starting of a voltage-constrained cycle takes place when the parallel plates have maximum capacitance  $C_{max}$ . With the help of battery or super capacitor the plates are charged to voltage  $V_0$ . The relative motion between plates was observe and they move slightly apart, while keeping the voltage constant. The energy obtained in voltage constrained cycle is given by the equation (1-6)

$$E = V^2(C_{max} - C_{min}) \quad (1-6)$$

Separation between plates increased and it results in reduced capacitance while keeping voltage constant. The transformation of mechanical energy to electrical energy occurs because of

decrease in capacitance value (g). The charge is transferred to load when plates are disconnected. In this cycle, the total energy given to the external circuit is equivalent to the net area encircled by the operation cycle curves in Figures 1-13 (a)–(e) and can be calculated with the maximum capacitance  $C_{max}$ , starting charging voltage  $V_0$ , and minimum capacitance  $C_{min}$  of plates during working of the system.

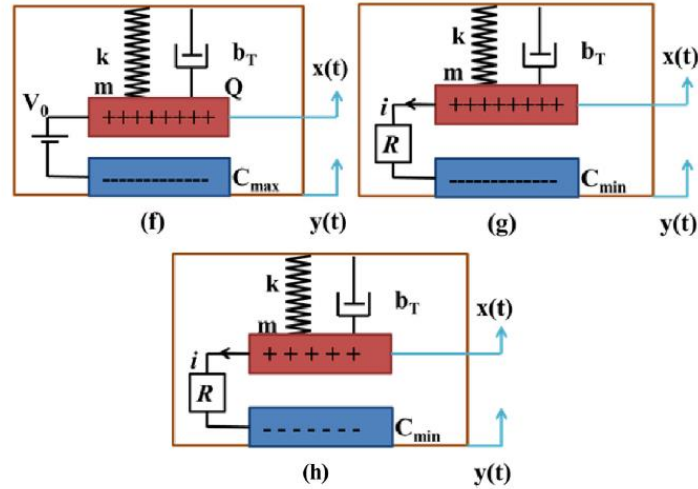


**Figure 1-15** Voltage-constrained cycle for EEHs [1]

(f) EEH's charging starts at  $C_{max}$ , (g) relative movement between the plates to achieve  $C_{min}$ , (h) charge removal from the EEH.

The system gives more output voltage than charge constrained cycle because of the larger charging period of the capacitor. When external bias is applied (f) it's kept constant on the capacitor plates while the displacement occurs. The discharging phase (g & h) starts when the capacitance reaches maximum value and the output circuitry is connected with the plates for extracting power. Voltage constrained cycle is a bit complex because it requires a constant voltage source for first half of the cycle.

## 1.8 Challenges in EEHs

With both types of EEHs, electret-based and electret-free, useful energy has been effectively produced and reported. However, there are still main issues related to EEHs. These challenges include reduction in size, optimization of power, EEHs designs that are able to transform enough power from low frequency vibrations, fabrication of non-resonant EEHs to deal with random vibrations, development of bandwidth harvester for broadband vibration, power generation from

small acceleration points, energy losses reduction because of parasitic capacitance, with respect to time electret stability, and low power external circuits development for EEHs charging and discharging.

Production of power from resonant-based energy harvesters is enhanced only at the resonant frequency; nevertheless, they produce very little power at anti-resonant frequencies. Hence, such high resonant frequency EEHs can't operate with low frequency vibrations. There is a condition for such EEHs to perform operation on low frequency and produce enough energy to power WSNs.

One of the other main issues related with vibration- based EEHs is the effective operation of these energy harvesters in the environment of random vibrations. These vibrations are usually narrowband or broadband and generally have narrow or wideband frequency range. Most EEHs are designed to operate proficiently at a specific frequency; their performance reduces considerably beyond that frequency. With increasing the harvester's bandwidth, the performance of harvesters can be altered for real random vibration environments [54].

There is also the issue of miniaturization. The smaller the harvester, more unstable it will be and will pose difficulty in operation. The size of the harvester and its reliability mainly depends on fabrication process used. Most process are not commercially available but provide better device dimensions and reliability. Due to this limit on selection of fabrication process, this project focuses on MetalMUMPs which is commercially available in MEMS fabrication.

## **1.9 Problem formulation**

In order to supply power to micro devices MEMS based energy harvesters are designed by different researchers to harvest ambient form of energy and the literature review in the field of vibration energy harvesting suggest that researchers have designed these generators mainly focusing on the fabrication technology, resonant frequency of the harvester, conversion mechanism, spring design, area of the device, and compatibility with existing CMOS fabrication technologies. These harvesters operate at a single frequency, but to utilize the maximum bandwidth of random vibrations one should consider the concept of multi degree of freedom systems which would operate at multiple frequencies [55]. The amplitude at resonant frequencies is usually high which is better for power extraction but the power in the adjoining frequency

spectrum is very low. This could be dealt with if the gain in those areas is to be made sufficient for the power to be of the desired value. However, the multi frequency concept can be used to harvest energy from wide range of frequencies. This concept is applied in resonators more specifically, coupled resonators which is a system consisting more than one proof mass attached to a substrate via mechanical springs and viscous dampers. The multi degree of freedom system will be further explained in detail in the coming chapters. The proposed device in this thesis is a result of this multi degree of freedom system concept.

## **1.10 Thesis outline**

In Chapter 1 introduction of Energy harvesters, need of energy harvesters and different transduction mechanisms such as piezoelectric, electromagnetic, solar and electrostatic are explored. Detailed literature survey is also included.

In Chapter 2 Concept of Three degrees of freedom (3-DOF) system is explained

In Chapter 3 Design and Analytical simulations for the proposed system are carried out using solid works and Matlab. Geometry of the proposed harvester is designed in SolidWorks. Mechanical parameters like damping, spring constant and displacement are given.

In Chapter 4 Finite Element Analysis is carried out using ANSYS 17.1 and COMSOL 5.2. The estimated output power, power density, excitation acceleration, resonant frequency and volume of the device are compared with prior work.

In Chapter 5 Conclusion and Future prospects are discussed

## CHAPTER 2: 3-DOF ELECTROSTATIC ENERGY HARVESTER

In this chapter working principle of electrostatic vibration energy harvester (EVEH) is discussed along with different configurations of electrostatic generators and their parameters. Concept of three degree of freedom (3-DOF) mass-spring system is given and based on previous work, best design topology is presented.

### 2.1 Concept of resonators

A resonator is a system consisting a single mass (Single DOF) attached with a fixed substrate through mechanical springs. The vibrations produced in the system by external force are dampened through viscous damping between mass and substrate, which is the coefficient of mechanical damping. These resonators are used to reduce the oscillations by absorbing vibrations in a system, e.g. shock dampers in cars.

Christopher Dyck in 1999 proposed a resonator which included two masses (2-DOF) attached with each other via mechanical spring [56]. The design comprised of two (1-DOF) systems with separate natural frequencies depending on the stiffness values of springs attached with the masses. A schematic of the Dyck design is shown in Figure 2-1.

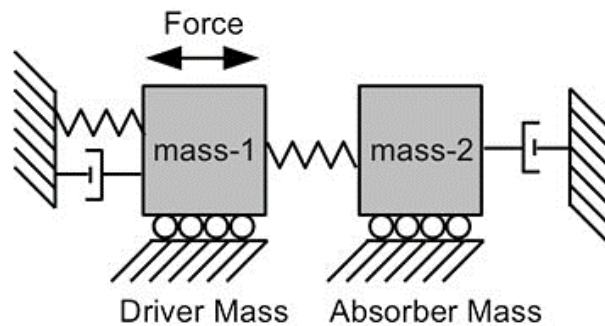


**Figure 2-1** schematic of resonator by Dyck [55]

The resonator showed best performance at resonance giving maximum displacement when operating frequency matches the resonance frequency of the system. This approach limits this device to certain areas where single frequency application is needed. The device is operated at anti-resonance frequency which is the value at anti-resonance peak as shown in Figure 2-2,

because at anti-resonance, the amplification in the displacement can be controlled by changing mass ratio i.e. ratio of driver mass to the absorber mass.

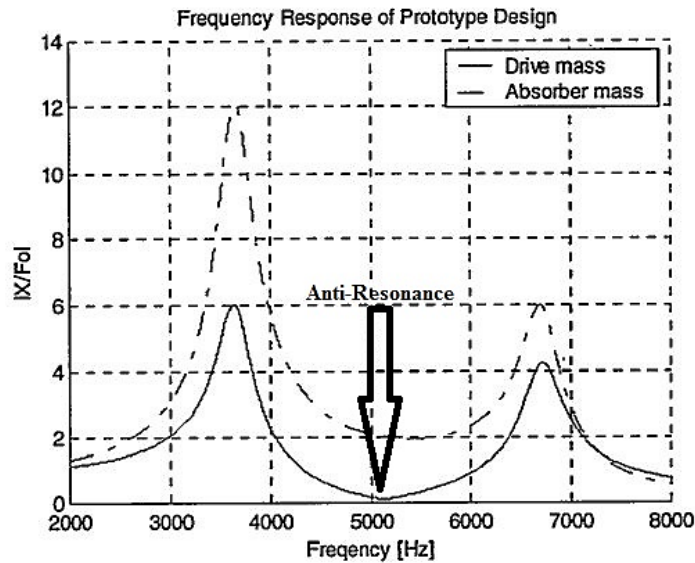


**Figure 2-2** Frequency Response of dual mass oscillator [56]

The dynamic behavior of the resonator is dependent on the design parameters such as spring stiffness and mechanical damping of the system. Dyck gave the fundamental approach on coupled resonators with operational frequency at resonance, but did not cater for the amplification issues due to changing mass ratio. The separation in the resonance frequencies is controlled by changing the mass ratio but this is not practical as mass value cannot be changed after fabrication and a smaller value of mass is required which is not a stable option.

Sahin in 2009 proposed a solution based on Dyck's design to incorporate some of the mechanical issues in the coupled resonators [57]. His device included an additional spring attaching the absorber mass with the substrate as shown in Figure 2-3. The design solved the problem for mechanical amplification dependent on mass ratio but still not gave solution to the issues arising due to mechanical imperfections in the device and drift in parameters due to environmental changes.

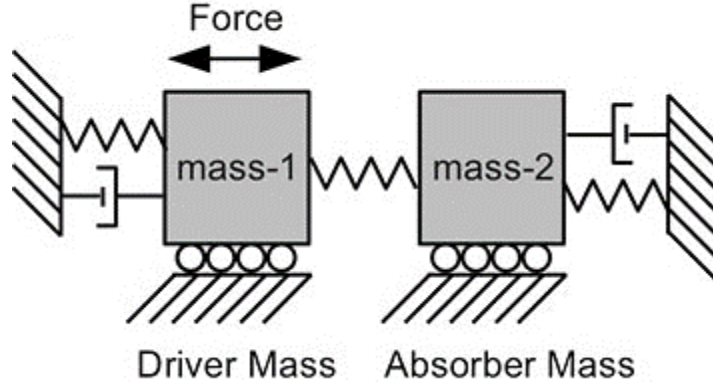


**Figure 2-3** schematic of resonator by Sahin (2009) [55]

A new model was proposed by E.A.Erismis in 2013 which consisted of three (1-DOF) systems coupled together by mechanical springs [55]. The schematic of the erismis design is shown in Figure 2-4.

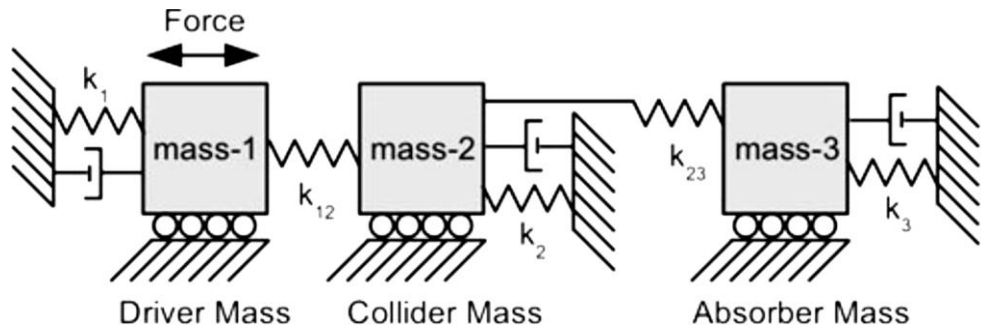


**Figure 2-4** Coupled resonator (3-DOF) concept by Erismis [55]

Erismis explained that by changing the value of spring stiffness attached with collider mass and absorber mass one can vary the length of the valley between resonance peaks. This can work best for wideband operational range in which sufficient gain is needed for power extraction cycle.

The equation of motion for the proposed design is given as follow [55]:

$$F_1 = k_1 X_1 + jwb_1 X_1 - m_1 w^2 X_1 + (X_1 - X_2) k_{12} \quad (2-1)$$

...

$$F_i + (X_{i-1} - X_i) k_{(i-1)i} = k_i X_i + jwb_i X_i - m_i w^2 X_i + (X_i - X_{i+1}) k_{i(i+1)} \quad (2-2)$$

...

$$F_n + (X_{n-1} - X_n) k_{(n-1)n} = k_n X_n + jwb_n X_n - m_n w^2 X_n \quad (2-3)$$

The analytical solution to these equations can be found as:

$$X_n = \frac{F_n + X_{n-1}k_{(n-1)n}}{D_n} \quad (2-4)$$

...

$$X_i = \frac{F_i + X_{i-1}k_{(i-1)i} + \sum_{l=i+1}^{l=n} F_l \prod_{m=i+1}^{m=l} \frac{k_{(m-1)m}}{D_m}}{D_i} \quad (2-5)$$

...

$$X_1 = \frac{F_1 + \sum_{l=2}^{l=n} F_l \prod_{m=2}^{m=l} \frac{k_{(m-1)m}}{D_m}}{D_1} \quad (2-6)$$

Where denominators are:

$$D_n = k_n + k_{(n-1)n} + jwb_n - m_n w^2 \quad (2-7)$$

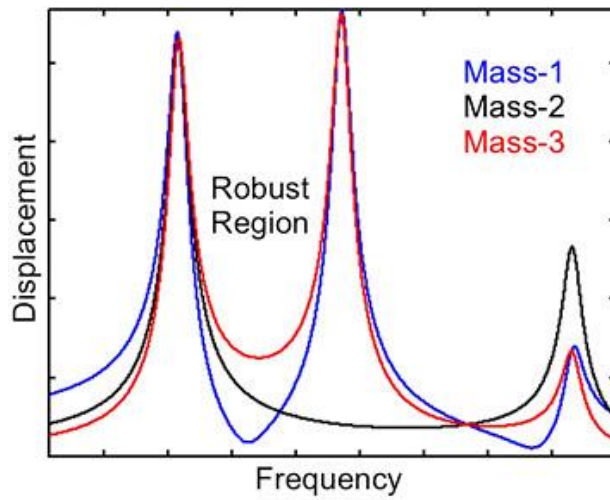
...

$$D_{(i)} = k_i + k_{(i-1)i} + k_{i(i+1)} + jwb_i - m_i w^2 - \frac{k_{i(i+1)}^2}{D_{i+1}} \quad (2-8)$$

...

$$D_1 = k_1 + k_{12} + jwb_1 - m_1 w^2 - \frac{k_{12}^2}{D_2} \quad (2-9)$$

It can be observed from the equations (2-4, 2-7) that the value of displacement for masses depends on spring stiffness as well as angular frequency of the system, where F is the force applied on the drive mass.



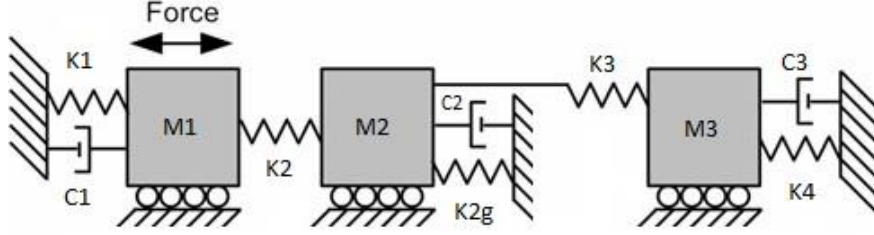
**Figure 2-5** Frequency Response of 3-DOF resonator [55]

Figure 2-5 explains the operation of a 3-mass system as proposed by Erismis [55]. The absorber mass has a robust region between two resonance frequencies. In this region, drive mass makes anti-resonance. Hence, there is dynamic displacement amplification between drive and absorber mass. The length of the robust region and the magnitude of this valley depend on the resonance frequency of collider mass, which can be varied by changing the spring constant that connects mass-2 to substrate. This spring is used to ground collider mass to the substrate. In addition to this, the position of the anti-resonance is easily controlled with the proposed 3-mass system. The position of the anti-resonance can be tuned by changing  $k_1$ , which connects mass- 1 to the substrate. This design gives dynamic amplification as well as robustness which is required for our proposed device.

## **2.2 Proposed 3-DOF system**

The dynamic energy harvester based on the Erismis concept, as discussed earlier, consists of three basic parts, mass (M), viscous damper (C) and suspension (K, spring). The mass is displaced by external periodic or constant force, due to the spring element, it tends to oscillate around its equilibrium position and this motion is used to convert mechanical energy in to electrical energy by attaching comb-drives with it.

For these generators to work in a confined space, displacement needs to be controlled by some force, dampers provide this reaction force which opposes the motion of proof or central mass. For wide range of frequencies and displacement amplification for lower mechanical vibration amplitudes 3-DOF dynamic energy harvester is chosen such that the transfer of energy from first mass to second and finally to the absorber mass will enable the harvester to generate power at multiple resonance frequencies. The concept of dynamic amplification is also used for optimization which is adjusting the tuning parameters such as spring constants or mass values in order to achieve desired response around selected frequencies.



**Figure 2-6** Proposed schematic for 3-DOF system [55]

Schematic of 3-DOF system is shown in Figure 2-6. In our case transduction mechanism (comb drives) is connected with the third mass which is the absorber mass.

### 2.3 Equations of 3-DOF system

The schematic representation of 3-DOF energy harvester is shown in Figure 2-6. In the proposed model  $M_1$  which is named as drive mass is connected directly to the substrate through spring  $k_1$ ,  $M_2$  known as collider mass is connected with drive mass by spring  $k_2$  and  $M_3$  is connected with  $M_2$  and substrate by springs  $k_3$  and  $k_4$  respectively. The design calls for another spring  $k_{2g}$  which grounds the  $M_2$ , the reasons for this are already discussed.  $Y_1$ ,  $Y_2$  and  $Y_3$  are displacements of  $M_1$ ,  $M_2$  and  $M_3$  respectively. Viscous-Damping coefficients are  $c_1$ ,  $c_2$  and  $c_3$ . The linear governing equations of motion under forcing function are written as:

$$f_1 = m_1 \ddot{x}_1 + c_1 \dot{x}_1 + (k_1 + k_2)x_1 - k_2 x_2 \quad (2-10)$$

$$0 = m_2 \ddot{x}_2 + c_2 \dot{x}_2 - k_2 x_1 + (k_2 + k_3 + k_{2g})x_2 - k_3 x_3 \quad (2-11)$$

$$0 = m_3 \ddot{x}_3 + c_3 \dot{x}_3 - k_3 x_2 + (k_3 + k_4)x_3 \quad (2-12)$$

The above equations can also be written in the matrix notation as

$$F = M\ddot{X} + C\dot{X} \quad (2-13)$$

Where  $X$  is the vector containing variables describing displacement,  $M$  is the matrix containing masses and  $K$ ,  $C$  are the matrices representing stiffness and damping respectively. For 3-DOF system all the matrices are of  $3 \times 3$  and for  $n$ -DOF system matrices will be of  $n \times n$ .

The system is solved using Matlab, for calculating natural frequencies and parameters describing the system. For a force  $F = f e^{j\omega t}$ , (2-4) will yield:

$$\begin{bmatrix} X_1 \\ X_2 \\ X_3 \end{bmatrix} = \begin{bmatrix} -\omega^2 M_1 + (k_1 + k_2) + j\omega C_1 & -k_2 & 0 \\ -k_2 & -\omega^2 M_2 + (k_2 + k_3 + k_{2g}) + j\omega C_2 & -k_3 \\ 0 & -k_3 & -\omega^2 M_3 + (k_3 + k_4) + j\omega C_3 \end{bmatrix} \quad (2-14)$$

The term  $(-\omega^2 M_1 + (k_1 + k_2) + j\omega C_1)$ ,  $(-\omega^2 M_2 + (k_2 + k_3 + k_{2g}) + j\omega C_2)$  and  $(-\omega^2 M_3 + (k_3 + k_4) + j\omega C_3)$  on the diagonal contribute to the displacement of the three masses. It can be observed that displacement in all the masses mainly depends on its respective spring which attaches it to the substrate, the angular frequency and the viscous damping which occurs between the mass and the substrate. The value of the displacement can be controlled by changing spring constants  $k_1$ ,  $k_{2g}$  and  $k_4$ , the stiffer the spring less movement it will allow. These three grounding springs are responsible for the displacement as well as natural frequency values of the three masses. These frequencies are calculated using the method explained below. The three masses are interlinked by the attaching springs,  $k_2$  and  $k_3$ , which plays important role when it comes to controlling the behavior of the masses between resonance frequency regions. The stiffer these springs are, the positions of the peak frequencies will come closer together creating a less wide region for operating between peaks.

The isolated resonance frequencies of the proposed energy harvester can be calculated using the equations mentioned below:

$$f_1 = \frac{1}{2\pi} \sqrt{\frac{K_1}{M_1}} \quad (2-15)$$

$$f_2 = \frac{1}{2\pi} \sqrt{\frac{K_{2g}}{M_2}} \quad (2-16)$$

$$f_3 = \frac{1}{2\pi} \sqrt{\frac{K_4}{M_3}} \quad (2-17)$$

These three frequencies can be observed by the three distinctive peaks of the frequency response graph in Matlab. The amplitude shown in the graph is for the un-damped model, the damping coefficients are neglected for the sake of easy calculation. The normalized steady-state response is shown in Figure 2-7

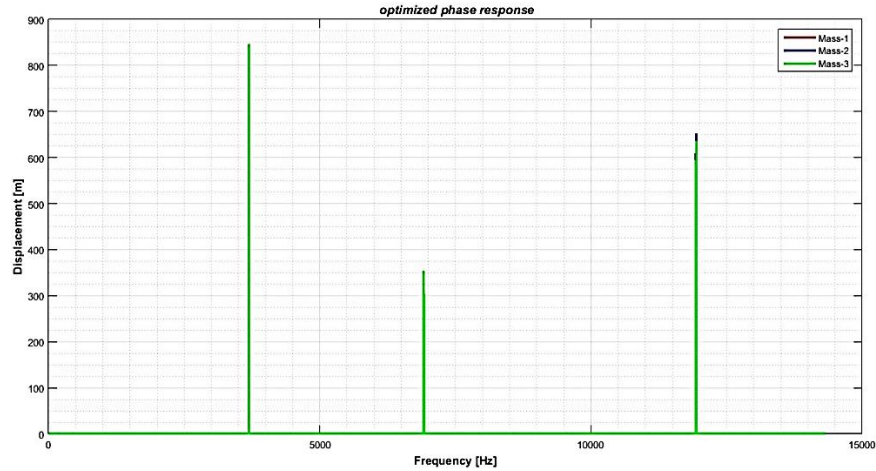


**Figure 2-7** Frequency response of un-damped system

External force is applied on drive mass as the above graph is drawn by taking the absolute of equations which means that amplitude of vibrations at some frequencies is negative which shows only that particular mass vibrates opposite to the applied force or out of phase with the applied force.

If the forcing frequency is close to any of the natural frequencies of the system, huge vibration amplitudes occur which is known to be resonance. Natural frequencies of the system along with tuning and amplification of displacements will be discussed in the later section of this chapter.

The output power of any inertial energy harvester directly depends on the displacements of drive and absorber masses, for electrostatic type of generator the combs gap can be varied according to these vibrations amplitude and that variation under electrostatic force results in the harvested power.

## 2.4 Calculation of natural frequencies by Eigen-value method

The resonant frequencies of the system can also be approximated by using Eigen-value method, which gives three Eigen values for the matrix system shown below. By equating the determinant of equation (2-9) to zero, three Eigen values are obtained

$$[K - \omega^2 M] = 0 \quad (2-18)$$

These values are then converted to the natural frequencies by dividing with  $2\pi$ . Values are listed in Table 2-1.

**Table 2-1** Natural frequencies of proposed system

<b>Frequency</b>	<b>Value (kHz)</b>
$\omega_1$	3.6938
$\omega_2$	6.9179
$\omega_3$	11.9378

The separation in three resonant frequencies is determined by changing mass ratio and frequency ratio.

## **2.5 Advantage of In-plane-overlap design**

Different scientists have compiled results of comparison among various topologies of EVEH. The comparison suggests the best choice by these parameters such as output power, operating frequency, fabrication method by biasing voltage, stability, output power density, and device volume [20]. In this report, the design is of in-plane type with variable overlap comb-drives for the following reasons:

- ❖ The in-plane gap converters can provide higher out-put power density.
- ❖ Mechanical Damping can be incorporated to avoid the collision between two electrodes
- ❖ Surface adhesion is negligible.
- ❖ More stable design compared to others.
- ❖ Variable-overlap design diminishes the problem of pull-in voltage.

## **CHAPTER 3: DESIGN AND ANALYTICAL SIMULATIONS OF THE PROPOSED DESIGN**

### **3.1 Overview**

The proposed design of 3-DOF electrostatic vibration energy harvester is explained in this chapter. Suspension along with damping for all three masses is discussed. Analytical simulations carried out in Matlab are also given.

### **3.2 Proposed design**

Electrostatic based Vibration energy harvester can convert mechanical energy in to useful electrical energy by varying the capacitance in the presence of bias voltage on the device. As discussed in Chapter 1 that electrostatic harvesters have advantage of integration with micro systems. These devices consist of proof mass along with transduction mechanisms for scavenging energy. The proof mass of the device should be selected in order to achieve the desired natural frequency, also by increasing the proof mass will result in decrease in its natural frequency and vice versa which is not desired in most cases because the devices having higher natural frequencies are impractical.

The design topology In-Plane overlap is selected as advantages of the proposed topology were discussed in Chapter-2. The device is designed using SolidWorks 2014. Schematic view of the device is shown in Figure 3-1. It consists of three masses (drive, collider and absorber mass), folded flexures as mechanical springs and comb-drives for power extraction. The electrostatic structure consists of movable and fixed comb fingers, movable fingers are attached with the absorber mass while fixed comb fingers are anchored directly on the substrate.

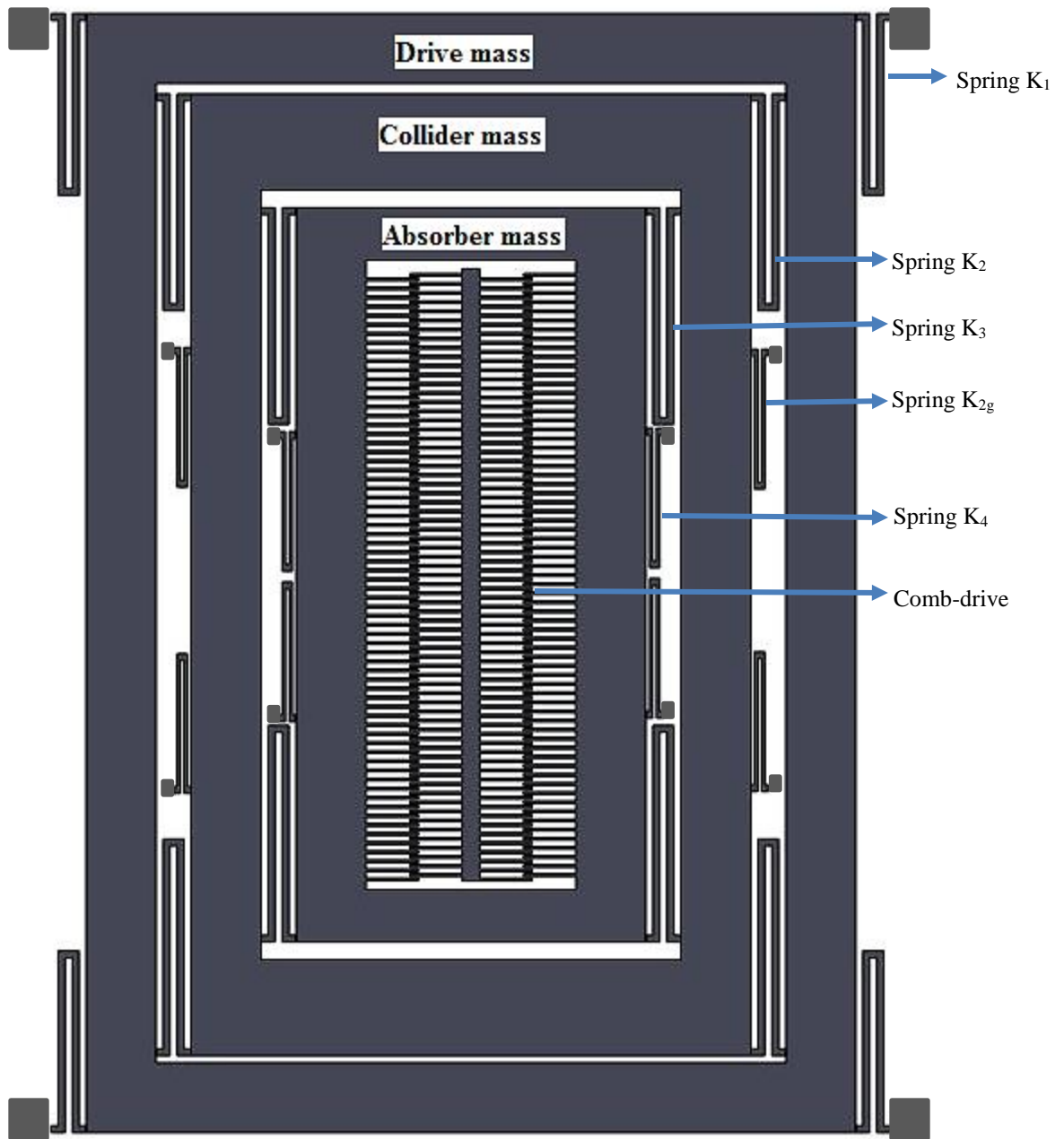


**Figure 3-1** Design of Proposed device

The dimensions of the device are  $3.2 \times 2.2 \text{ mm}^2$  with  $20 \mu\text{m}$  structural thickness. The EVEH can harvest maximum electrical power at maximum capacitance and this is achieved through large displacement of proof mass. The 3-DOF device incorporates 3 masses which provides better concept for dynamic motion amplification. Drive mass or outer mass ( $M_1$ ) is suspended over the substrate by four double folded flexures, collider mass is boxed within drive mass with similar flexures and absorber mass is connected to collider mass which is then grounded with the substrate with additional springs. To deposit initial charge on the comb drives bias voltage is applied on fixed and moving combs of the device. Geometrical parameters of the device are selected according with design rules of Metal MUMPs standard fabrication process with minimum feature size  $8\mu\text{m}$ . Finite element analysis is carried out in ANSYS 17.1 and COMSOL 5.2, used to provide physical modeling and verification of the MEMS based structure.

Power management control circuitry will be needed as the output power of electrostatic converters is not sufficient enough to operate the device directly. There is a need for power converter and storage elements, but for the harvester in this thesis only transducer part is discussed. The structure can be first charged by external biasing source and again when proof mass is at extreme position because at that point capacitance value is maximum. Then the device is disconnected when proof mass is moving towards mean position in order to keep the charges on the electrodes and this simultaneous switching will occur in each mechanical cycle of operation. All this can be controlled by power management and control circuitry. In order to achieve the maximum power from the harvester comb drives are attached with absorber mass having its motion amplified through dynamic amplification factor. All combs are utilizing in-plane overlap type configuration.

### **3.3 Mechanical design elements of proposed device**

In this section the mechanical parts of energy harvester which includes Proof mass, Design of suspension system and damping will be discussed.

The size of the energy harvester can be selected according to the available space on specific application. As drive mass can be fixed as per device size and the absorber mass can be used for tuning purpose in order to obtain the desired natural frequency of the device.

### 3.3.1 Suspension design

At micro-scale coiled springs are not possible to fabricate therefore beams with one end being fixed are used as a spring structure at micro level these micro beams are used to hold proof mass on the substrate. The stiffness value of the springs can be chosen according to desired operating frequency of the device. The stiffness depends on the width, thickness and length of the beams. Different types of spring with different shapes are available for micro suspension such as folded flexure, crab leg, serpentine and bent beams [58-61] as shown in Figure 3-2.

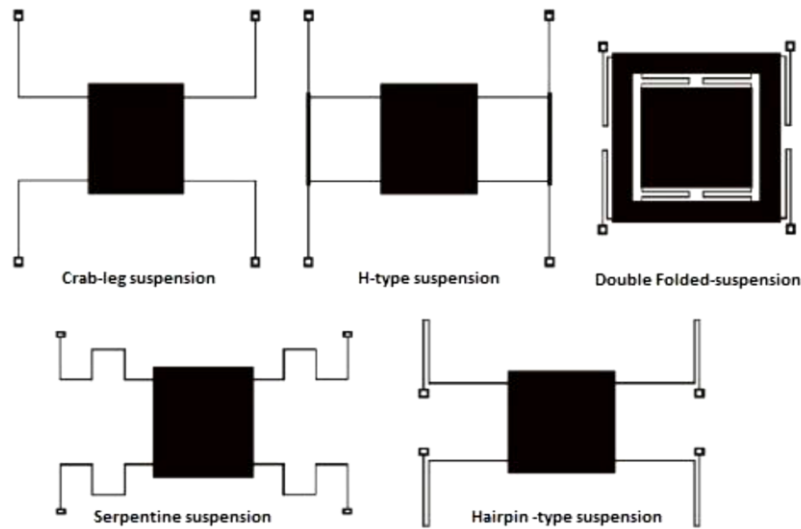


**Figure 3-2** Different suspension designs [61]

For translator or linear motion, rigid body motion will be strictly along one axis and the folded flexure are mainly used due to their minimum quadrature error and suspension efficiency [59]. In folded flexures every beam used is modeled as fixed guided beam and the spring constant for folded flexure is given by [62].

The designing of springs for microstructure can be done according to selected natural frequency in order to match the input frequency provided by source because mass of the system is determined according to available space. The flexures should be hard enough in out of plane deflections in order to maximize the proof mass deflection only in the desired plane, which is in plane motion in this project and springs should be less hard along in plane motion. As the device layout is shown in Figure 3.1 which consists of eight folded flexures with tow masses known as drive and absorber mass one of the folded flexure is shown in Figure 3-3.

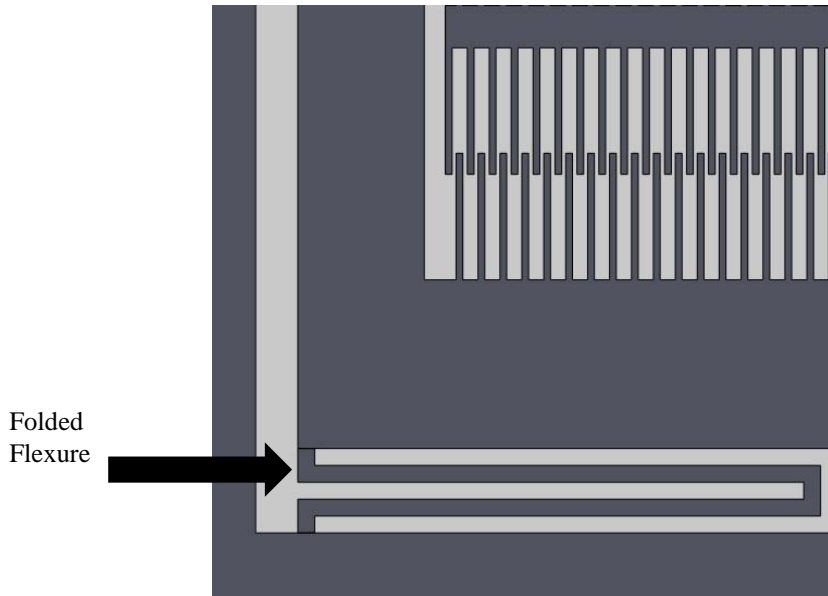


**Figure 3-3** Folded flexure used in proposed device

The spring constant for folded flexure moving within plane is giving by equation 3.1

$$K = \frac{2Etw^3}{L^3} \quad (3-1)$$

Where:

E is the Young's modulus of the material (Nickel in our case).

L is the beam length of flexure.

t is the beam thickness of flexure.

w is the beam width of flexure.

The material property that is young modulus and thickness of the device cannot be varied for the achievement of desired stiffness value so width and length can be changed in order to get the desired stiffness.

### 3.3.2 Damping

Damping is the opposing force acting on the structure during its motion. As in MEMS based structure damping arises due to friction of fluid present between proof mass moving inertial part of the device and the fixed surface on which proof mass is suspended.

The dominant damping at micro-scale electrostatic structure is the viscous damping. The viscous effects of the air molecule between the stationary and moving fingers of comb drive is known as squeezed film damping as shown in Figure 3-4. The Hagen-Poiseuille law is used to approximate the squeeze film damping between two parallel plates as demonstrated by equation 3-2 [63].

$$C_{squeez} = \mu \frac{7AZ^2}{y^3} \quad (3-2)$$

Where  $y$  is the air gap between fixed and moving comb plate,  $A$  is the area of the respective mass and  $Z$  is the gap between substrate and seismic mass.

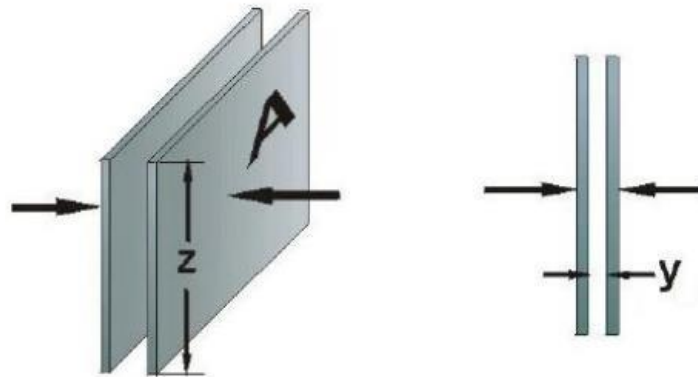


**Figure 3-4** Squeeze film damping between electrodes [63]

The viscous effect found between the seismic – mass and the base substrate is known to be Couette-flow damping as shown in Figure 3-5. Couette-flow damping can be estimated by the equation (3-3) [63]

$$C_{couette} = \frac{\mu A}{y} \quad (3-3)$$

Where,  $A$  represent the overlap area,  $\mu$  represents the air viscosity which is equal to  $1.8 \times 10^{-5}$  Pascal-Secondo at room temperature.

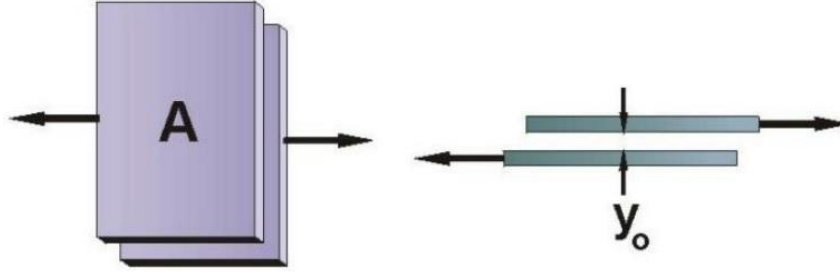


**Figure 3-5** Couette-flow damping between electrodes [63]

Therefore for the proposed EVEH the total damping is the sum of Couette-flow and squeezed-film damping as given by equation (3-4).

$$C = \mu \frac{7NL_f t^3}{y^3} + \frac{\mu A}{y} \quad (3-4)$$

Where  $N$  represents the total number of comb in a device,  $L_f$  and  $t$  represents the finger length and thickness respectively and  $y$  is the nominal gap between fixed and movable fingers.

The parametric optimization of the harvester can be done to locate the frequencies of 3 DOF systems and amplification of mass displacements. The steady state response of a system is shown in Figure 3.7 for first mode of frequency, which represents the displacement amplitudes of drive mass and absorber mass and phase response at dual mass first natural frequency of 3.9 kHz as it is concluded from phase response that for first natural frequency resonance occurred when all masses are in-phase that is moving in same direction. Figure 3.8 represents the amplitude of drive, collider and absorber mass. As at high frequency amplitude is low which cannot produce electrical power from such a small displacement of proof masses, therefore displacement amplitude for these low level displacements can be ignored. The phase response at second and third resonant frequency shows that both drive and absorber are out of phase with each other in other in words both are moving in opposite directions. The separation between first mode resonance frequency and second mode resonance frequency can be varied by mass ratio  $\mu$  which is  $(m_1/m_2)$  and  $(m_2/m_3)$ .

The amplification of absorber mass displacement amplitude also depends on the ratio of masses  $\mu$  and majorly on the ratio of system isolated natural frequencies  $\sigma$ . The system isolated resonant frequencies are given by  $\omega_1$ ,  $\omega_2$ , and  $\omega_3$  respectively and  $\sigma$  is the ratio of isolated system

frequencies and amplification of mass can be achieved by making  $\sigma$  as much larger as possible with in a given area.

### 3.4 Design parameters of proposed device

The parameters of the proposed device are selected based on the parametric optimization done in previous section in order to achieve the desired natural frequency, excitation acceleration for which desire displacements of drive and absorber masses can be achieved to harvest maximum electrical power from ambient vibrations. As electrostatic type of generators consists of comb drives so that in the available device volume optimum displacement amplitudes will be required which define the number of comb drives attached with the masses. The design parameters were subjected to a loop where all dimensions were kept constant except one, which is varied in the loop until maximum displacement is achieved. The optimal parameters are chosen to scavenge maximum energy and are shown in Table 3-1.

**Table 3-1** Design parameters of the proposed device

<b>Design Parameter</b>	<b>Value</b>
Drive mass ( $M_1$ )	$4.0406e^{-07}$ kg
Collider mass ( $M_2$ )	$3.0260e^{-07}$ kg
Absorber mass ( $M_3$ )	$2.2286e^{-07}$ kg
Stiffness of spring $K_1$	222.87 N/m
Stiffness of spring $K_2$	359.17 N/m
Stiffness of spring $K_3$	560.64 N/m
Stiffness of spring $K_{2g}$	159.64 N/m
Stiffness of spring $K_4$	118.23 N/m
Damping between $M_1$ and substrate ( $c_1$ )	$2.0544e^{-04}$ Ns/m
Damping between $M_2$ and substrate ( $c_2$ )	$1.5385e^{-04}$ Ns/m
Damping between $M_3$ and substrate ( $c_3$ )	$1.3430e^{-04}$ Ns/m
Gap between comb fingers ( $Z_1$ )	$8 \mu m$
Overlapping length of fingers ( $L_f$ )	$25 \mu m$

The energy harvester is designed for high excitation frequency as discussed earlier in chapter 1 as three mass systems have three peaks at mode-1, mode-2 and mode-3 respectively. Third mass gives quite large displacement as compared with other two masses thus this mass is selected to

attach the combs with. These high frequency spectrums make the device limited to use in specific areas only such as acoustics or high frequency noise generators.



### 4.3.1 Material properties

Nickel is used as a structural material which is flexible and hard in nature. The density of Nickel is  $8.9 \text{ g/cm}^3$  and Young's modulus 219 GPa [64, 65].

### 4.3.2 Optimization

Optimization was carried out in Matlab. The device parameters were found in order to achieve maximum displacement in Mass-3 with which combs are attached. The length and width of springs and area of masses were subjected to looped trial-based-Method, as explained earlier in order to obtain the desired results. Figure 4-2 and 4-3 shows displacement profile before and after optimization.

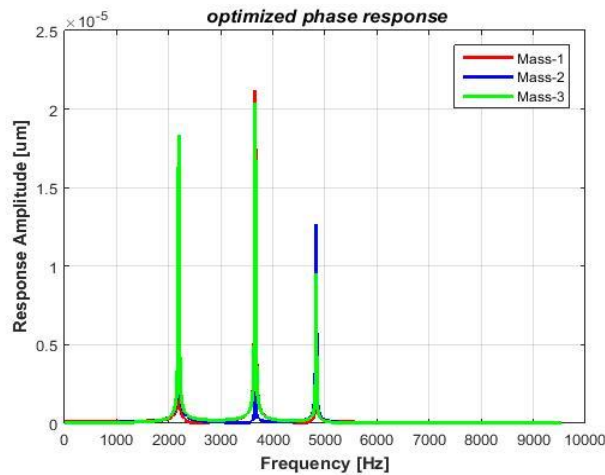


**Figure 4-2** Un-damped frequency response in Matlab for the proposed design

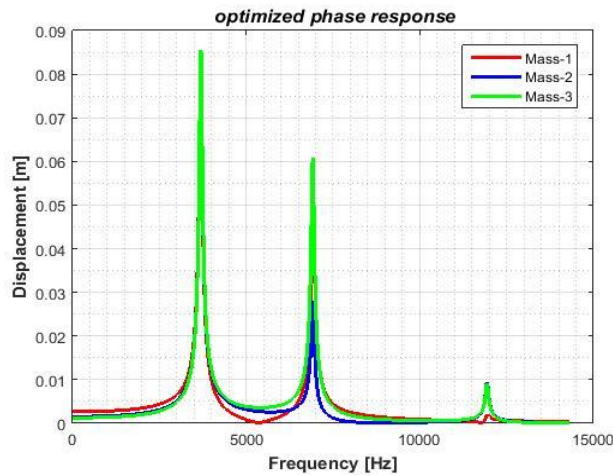


**Figure 4-3** Damped frequency response in Matlab for the proposed design

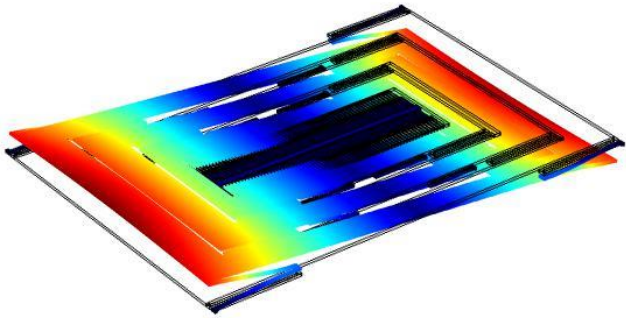
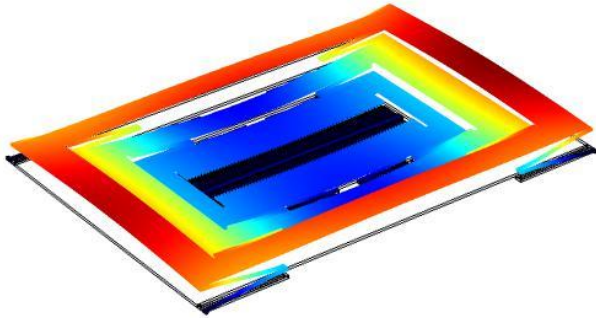
### 4.3.3 Modal analysis in ANSYS and COMSOL

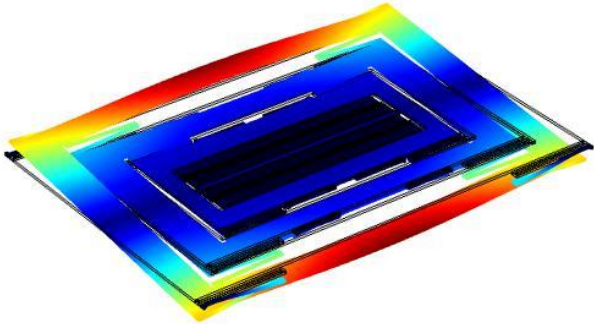
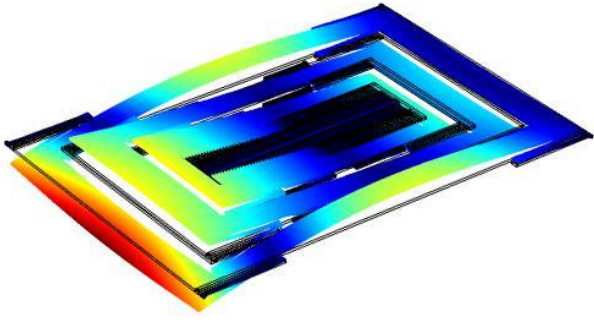
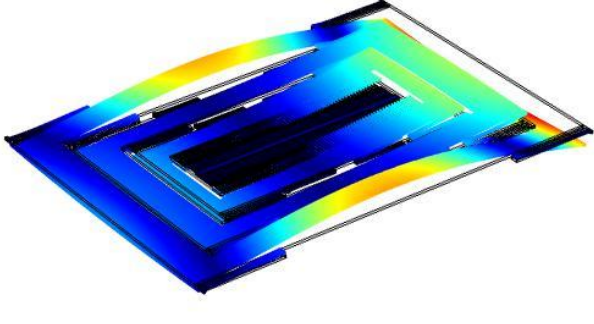
Modal analysis was done to find the natural frequencies and associated modes of 3-DOF energy harvester. The natural frequency at 1<sup>st</sup> mode of vibration was analytically calculated to be 3926 Hz and natural frequency numerically calculated in modal analysis is 3974 Hz, therefore percentage error of less than 1% arises which was due to difference between physical level modeling and analytical modeling. The first six modes of natural frequencies are also given in Table 4.1

**Table 4-1** first six modes of natural frequencies

Mode Number	Natural frequency (Hz)	
	ANSYS 17.1	COMSOL 5.2
1	3422	3533
2	3969	3985
3	4021	4071
4	5124	5324
5	6285	6380
6	6487	6401

**Table 4-2** Different mode shapes explained

Modes	Mode Shape	Comments
Mode - 1		All three masses are moving out of the plane together
Mode - 2		Masses are moving in plane
Mode - 3		All masses are moving out of the plane but out of phase with mass-1

<p>Mode - 4</p>		<p>Masses are moving out of the plane with zero displacement in mass-3</p>
<p>Mode - 5</p>		<p>All the masses are moving out of plane with simultaneous motion in phase and out of phase with each other</p>
<p>Mode - 6</p>		<p>Similar to mode-5 with zero displacement in mass-3</p>

The associated mode shapes are shown in above Table. Feasible mode of vibration for operation is clearly mode 2 because the device move in-plane having displacement in all three masses. The response of force applied on the device is measured using harmonic analysis; Figure 4-4 shows the available modes while figure (k) shows the mode-2 under operation

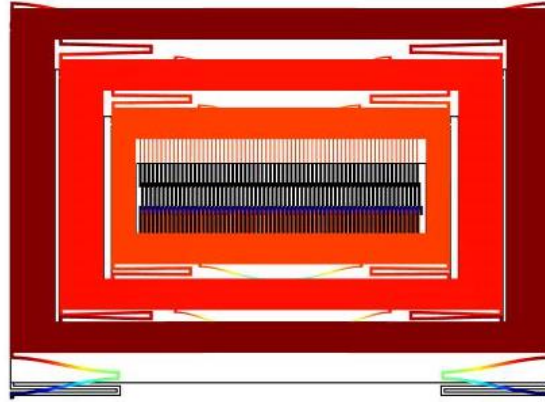


**Figure 4-4** Second mode shape in COMSOL

For a load of 0.1g the displacement in Mass-3 was calculated to be few microns. This is in accordance with the result obtained by numerical method using Matlab. The required gain is somewhat low but can be increased through further optimizing the device's and fabrication parameters such as mass length or width. No mechanical stoppers are introduced in this design because it only covers the modal and FEM analysis on a fundamental level.

#### 4.3.4 Harmonic analysis in ANSYS and COMSOL

A harmonic analysis is carried to determine the displacements of absorber mass for 0.1 g time varying load. The comb drivers are attached with absorber mass in order to harvest energy from dynamic amplification factor. Different shapes of displaced design are shown along with analytical readings. The COMSOL module also incorporates the damping in the form of damping ratios i.e.  $\xi_1$ ,  $\xi_2$  and  $\xi_3$  for drive, collider and absorber masses respectively. The damping ratios are calculated using (4-1)

$$\xi_i = \frac{c_i}{2M_i f_i} \quad (4-1)$$

Where,

$c_i$  is the damping coefficient for the viscous dampers

$M_i$  is the respective mass

$f_i$  is the respective resonance frequency at which damping ratio is required

The ratios for mass-1, mass-2 and mass-3 are calculated to be 0.0108, 0.0111 and 0.0131 respectively. The Rayleigh damping coefficients  $\alpha$  and  $\beta$  are used in ANSYS. The damping ratio  $\xi_3$  is used to further calculate  $\alpha$  and  $\beta$ , which is then used to analyze the device under damped conditions in ANSYS.

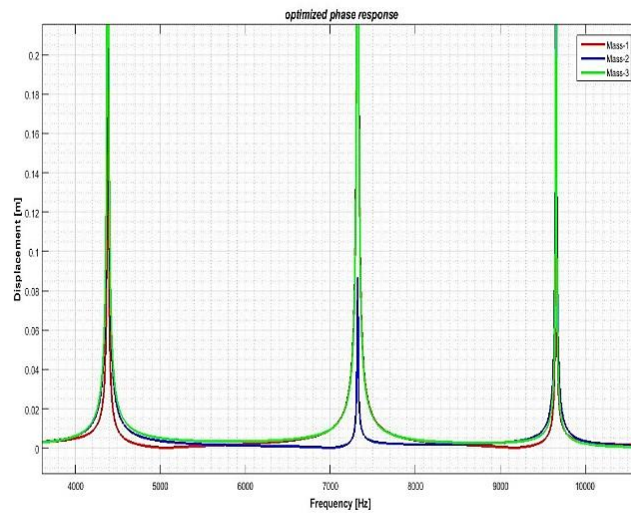


**Figure 4-5** phase response of un-damped system in Matlab

In Figure 4-5 the meshed design is subjected to fixed load at 0.1g in Matlab and the displacement curve is obtained for un-damped model. The three peaks are shown in the Figure are normalized.

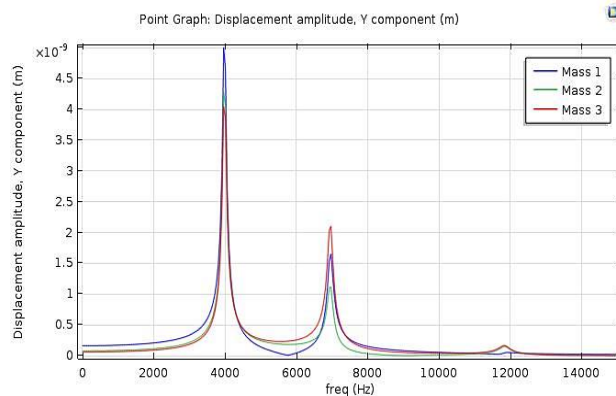


**Figure 4-6** phase response of damped system in COMSOL 5.2

Figure 4-6 shows model with same boundary conditions, with damped conditions i.e.  $\xi_3$  for absorber mass.

The proposed harvester showed promising results both in modal and FEM analysis which was the scope of this research. All the results are calculated for both damped and un-damped scenarios. The FEM Analysis is ANSYS required  $\alpha$  and  $\beta$  calculations in order to subject the design to damped conditions under load.

The values for  $\alpha$  and  $\beta$  are calculated using the following equations,

$$\alpha = 2 \xi_3 \frac{\omega_1 - \omega_2}{\omega_1 + \omega_2} \quad (4-2)$$

$$\beta = \frac{2 \xi_3}{\omega_1 + \omega_2} \quad (4-3)$$

Where,

$\omega_1$  is the first angular frequency

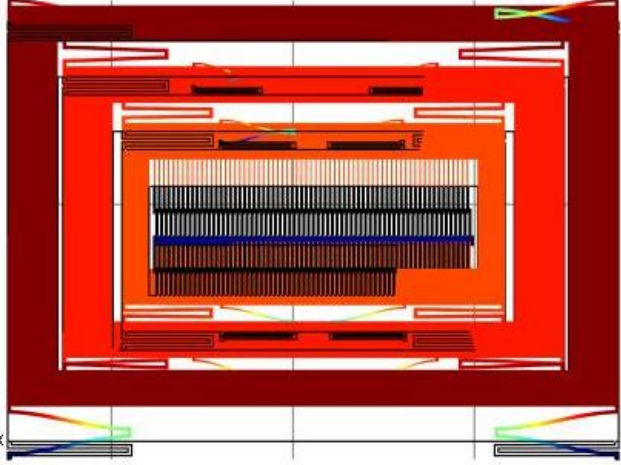
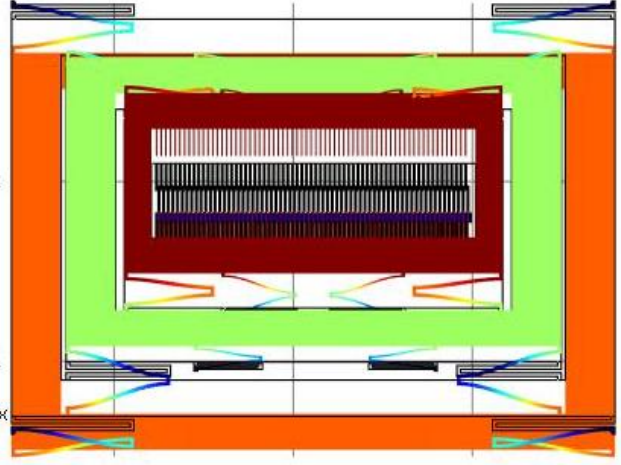
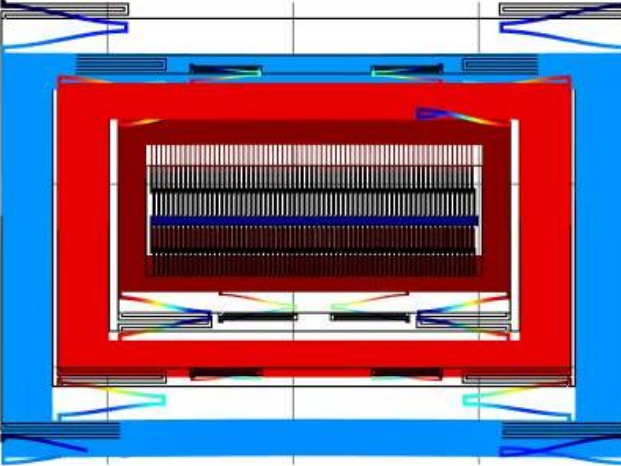
$\omega_2$  is the second angular frequency

$\xi_3$  is the damping ratio for mass-3

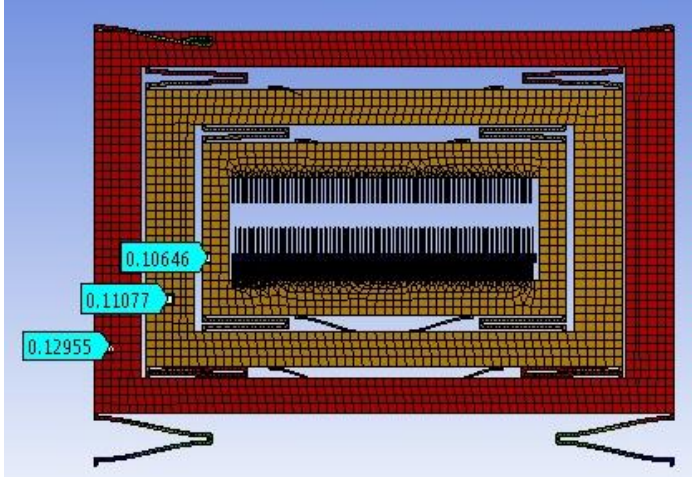
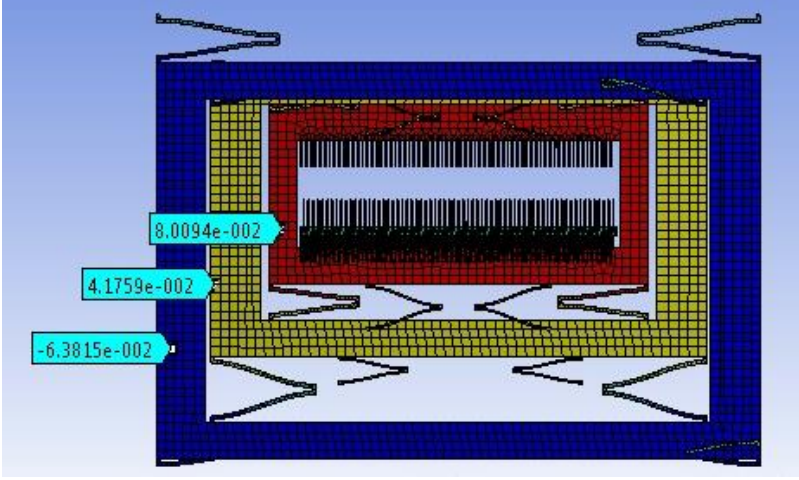
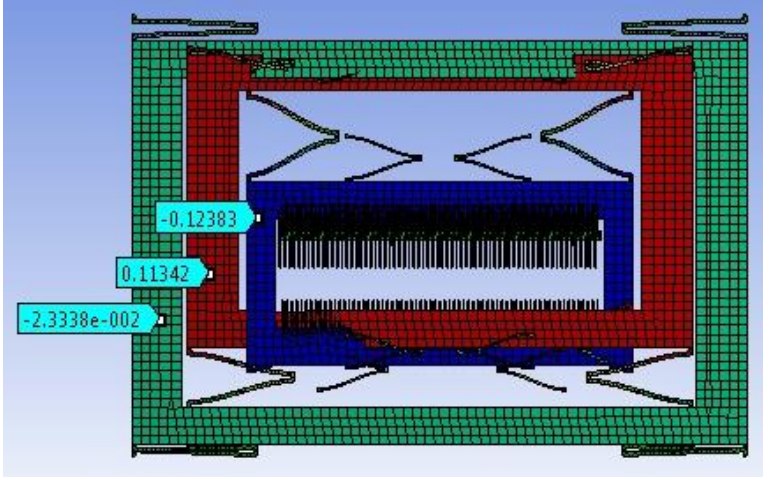
$\alpha$  and  $\beta$  comes out to be  $-970$  and  $2.81e^{-7}$  respectively. The values are calculated for  $\xi_3$  only because the damping coefficient associated with mass-3 comes into effect and incorporating  $\xi_1$  and  $\xi_2$  will become difficult in solving equations. The software uses separate single values for  $\alpha$  and  $\beta$  thus only damping due to combs attached with mass-3 is important and we can neglect the other damping coefficients in this analysis, which could be integrated later on in future work.

The Table 4-3 and 4-4 shows the displacement profile of the device at all three peaks. Results are compiled for harmonic response analysis in both ANSYS and COMSOL. The displacement values for each mass along with gain and output power is listed in Table 4-5 and 4-6.

**Table 4-3** displacement profiles of the device in COMSOL

<b>Frequency (Hz)</b>	<b>Displacement Profiles COMSOL 5.2</b>
<b>3963</b>	 A finite element mesh of a rectangular device structure. The displacement profile is shown with a color scale from blue (low displacement) to red (high displacement). The highest displacement is concentrated in the outermost frame, which is colored dark red. The inner components, including a central array of vertical lines, show significantly lower displacement, indicated by blue and green colors.
<b>6973</b>	 A finite element mesh of the same device structure. The displacement profile shows a different distribution. The central array of vertical lines and the inner frame are now colored red, indicating high displacement. The outer frame is colored orange and yellow, indicating lower displacement compared to the 3963 Hz case.
<b>11839</b>	 A finite element mesh of the device structure. The displacement profile shows the highest displacement in the central array and inner frame, which are colored red. The outer frame is colored blue, indicating the lowest displacement in this configuration.

**Table 4-4** displacement profiles of the device in ANSYS

Frequency (Hz)	Displacement Profiles ANSYS 17.1
3974	
7028	
12020	

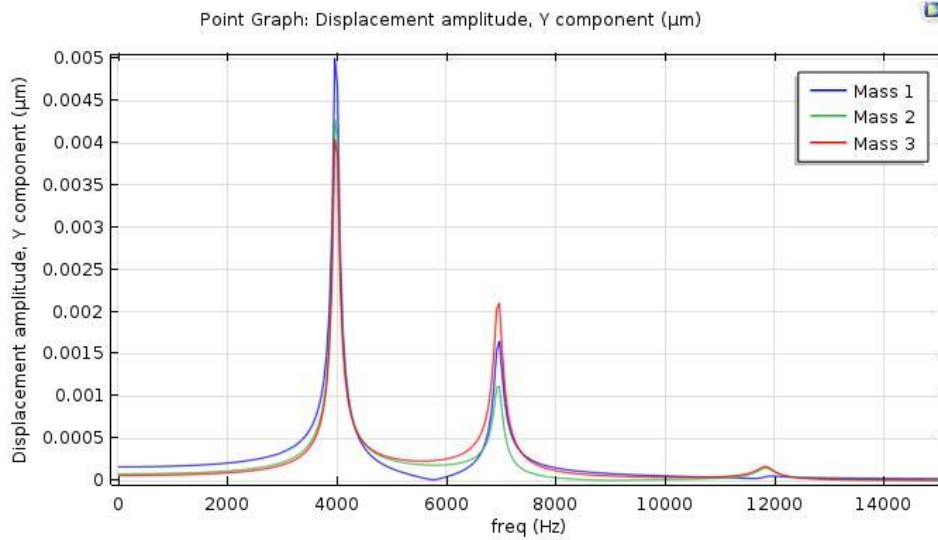


**Figure 4-7** Frequency response graph in COMSOL

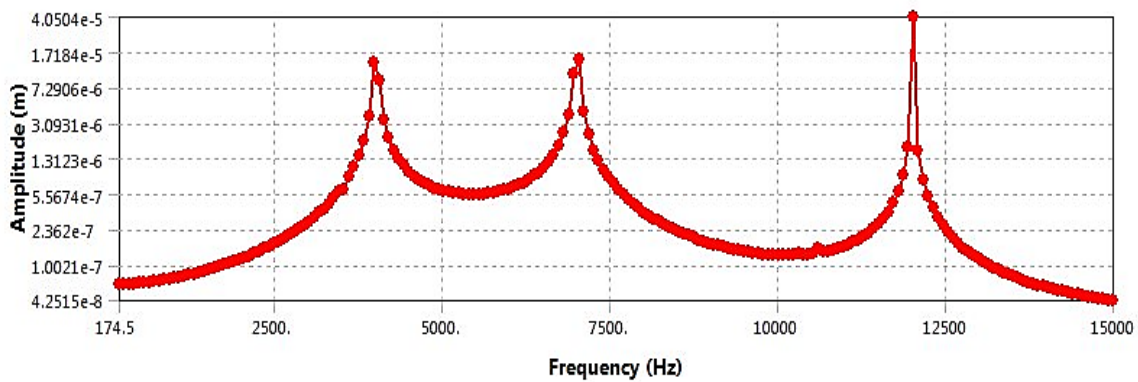


**Figure 4-8** Frequency response graph in ANSYS

The comparison among physical and analytical simulations is shown in the Table below. The difference in values occurred due to variation of methods used to obtain numerical and physical level values and results.

**Table 4-5** Amplitudes of masses at peak frequencies

Method	Input g	Amplitude at $f_1$ ( $\mu\text{m}$ )			Amplitude at $f_2$ ( $\mu\text{m}$ )			Amplitude at $f_3$ ( $\mu\text{m}$ )		
		M1	M2	M3	M1	M2	M3	M1	M2	M3
Analytical	0.1	0.081	0.082	0.083	0.05	0.025	0.06	0.0021	0.0085	0.0091
ANSYS	0.1	0.1295	0.1107	0.1064	0.006	0.004	0.008	0.0023	0.1134	0.1238
COMSOL	0.1	0.005	0.0042	0.0041	0.0016	0.0011	0.0021	0.00002	0.00014	0.00016

**Table 4-6** Gain and output power at peak frequencies

Method	Input g	Gain f1 and f2 (μm)	Gain f2 and f3 (μm)	Output Power f1 (nW)	Output Power f2 (nW)	Output Power f3 (nW)	Output Power between f1 and f2 (nW)	Output Power between f2 and f3 (nW)
Analytical	0.1	0.004	0.0009	4.29	5.3	1.43	0.6	1.2
ANSYS	0.1	0.4	0.1	5.61	0.7	19.73	27.3	13.2
COMSOL	0.1	0.00025	0.00004	0.21	0.19	0.025	0.017	0.0053

#### 4.4 Output Power

Power of electrostatic type energy harvester is estimated according to equation 4-3 which was also discussed in Chapter 2 with detail proof. Power is the rate of change of energy depends on change in capacitance under bias voltage. In the case for electrostatic transducer or harvester, however further capacitance depends on the structural material, geometrical parameters like length, width and thickness and more importantly the displacement of the structure which defines the minimum and maximum capacitances.

$$P = 2E_c \frac{\omega}{2\pi} \tag{4-3}$$

Where  $\omega$  is angular frequency of the harvester and the factor of 2 represents that in one mechanical cycle two electrical cycles obtained. The maximum electrical power is harvested at resonant frequency. The numerically calculated power from the comb drives which are attached with absorber mass is shown in Figure 4-9.

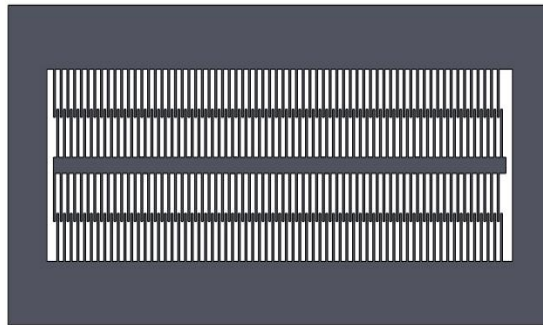


**Figure 4-9** Comb-drives attached with absorber mass

In the proposed design comb drivers are attached with absorber mass which means it's capable of producing power from ambient vibration with Amplified results. The total power of 4.2 nW is calculated.

#### 4.5 Power Density

Power density is defined as the rate of transfer of energy in a unit volume or per unit volume per acceleration. It is a parameter to measure energy harvesting device's performance with respect to device volume. The proposed energy harvester had dimensions of  $3.2 \times 2.2 \times 0.02 \text{ mm}^3$  so the power density of a harvester is  $0.0032 \text{ mW/cm}^3\text{g}^{-2}$ .

#### 4.6 Comparison with Previous Work

The proposed design is compared with previous work and the output power having such a small device size and power density achieved for the proposed harvester is greater among all prior designs. Table 4-5 represents the detailed comparison of the proposed design and the harvester's previously designed using electrostatic energy harvesting mechanism. The design is able to harvest  $2.4 \mu\text{W}$  but with such a small mass and dimensions natural frequency of the harvester lies within the spectra of high frequency sources of vibration which are rare in environment but could be found in areas of acoustics and high speed machines like airplanes and electronic oscillators.

**Table 4-7** Comparison with previous work

Ref	f (Hz)	Mass (g)	Acceleration ( $\text{ms}^{-2}$ )	Volume ( $\text{mm}^3$ )	System	Power ( $\mu\text{W}$ )	Power density ( $\mu\text{W}/\text{mm}^3\text{g}^{-2}$ )
[67]	179	0.06	0.3	0.15		0.03	0.2407
[68]	110	0.267	20	0.484	OPGC	20	0.0107
[69]	150	0.066	10	0.042	IPGC	2.2	0.052
[70]	109	0.066	2.5	0.038		1.3	0.547
[71]	28	0.5	5	0.305		1.5	0.0197
[19]	96	0.07	9.8	0.29	OPGC	0.15	0.00052
[66]	63	0.1	20	0.305	IPO	1	0.00082
<b>This work</b>	<b>3900</b>	<b>9.4 mg</b>	<b>0.98</b>	<b>0.140</b>	<b>IPO</b>	<b>4.2nW</b>	<b>0.0032</b>

## CHAPTER 5: CONCLUSION AND FUTURE PROSPECTS

### 5.1 Conclusion

The novel design concept utilizing three degrees of freedom is presented in this project, In order to harvest maximum power comb drivers are attached with absorber mass in which dynamic amplification occurred. The literature survey relating electrostatic type energy harvester shows that the best configuration of comb drives is in-plane overlap. Our design incorporates this type of configuration with comb drives in this device. Due to unavailability of fabrication facility in our country low cost standard fabrication process MUMPs provided by MEMSCAP is selected, usually three types of processes are provided by MEMSCAP those are SOIMUMPs, PolyMUMPs and MetalMUMPs all differs with each other in a material usage for structural layer and minimum feature sizes in this project MetalMUMPs process was selected with minimum feature size of  $8 \mu m$  and thickness  $20 \mu m$ . The area of the proposed device is  $3.2 \times 2.2 \text{ mm}^2$  and overlap length of the combs attached is  $25 \mu m$ . The mass of the device is  $9.4 \text{ mg}$  with device volume of  $0.140 \text{ mm}^3$  and total harvested power was  $4.2 \text{ nW}$  having power density of  $0.0032 \text{ mW/cm}^3 \text{ g}^2$ .

### 5.2 Future Work and Recommendations

This design can be tested with addition of power management and control circuitry for charge constrained cycle. As the proposed harvester utilizes the charge constrained cycle in which switching can be done in every mechanical cycle to deliver power at storage element so power electronic circuitry will be required to perform such switching. Due to low output power of the harvester it is not possible to directly deliver power to load, therefore storage or energy buffer will be needed in order to supply continuous power to load the power control and management scheme is as shown in Figure 5-1.

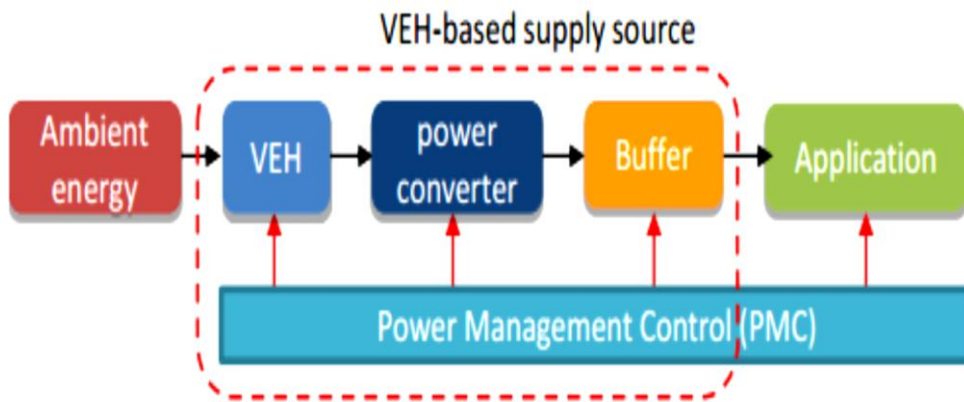


**Figure 5-1** Block diagram for power management circuitry [20]

The major drawback of the proposed device is usage of external biasing source. So in order to avoid external biasing source it is recommended to use electret layer based electrostatic harvester in which biasing voltage can be provided by electret layer which can be charged once during fabrication of a device and it have ability to hold those charges for a very long time period.

## REFERENCES

- [1] F.U. Khan, M.U. Qadir, State-of-the-art in vibration-based electrostatic energy harvesting, *Journal of Micromechanics and Microengineering*, 26(2016) 103001.
- [2] P. Kamalinejad, C. Mahapatra, Z. Sheng, S. Mirabbasi, V.C. Leung, Y.L. Guan, Wireless energy harvesting for the Internet of Things, *IEEE Communications Magazine*, 53(2015) 102-8.
- [3] M. Stordeur, I. Stark, Low power thermoelectric generator-self-sufficient energy supply for micro systems, *Thermoelectrics, 1997 Proceedings ICT'97 XVI International Conference on, IEEE1997*, pp. 575-7.
- [4] D. Le Gall, MPEG: A video compression standard for multimedia applications, *Communications of the ACM*, 34(1991) 46-58.
- [5] S.P. Beeby, M.J. Tudor, N. White, Energy harvesting vibration sources for microsystems applications, *Measurement science and technology*, 17(2006) R175.
- [6] S. Roundy, P.K. Wright, K.S. Pister, Micro-electrostatic vibration-to-electricity converters, *ASME 2002 International Mechanical Engineering Congress and Exposition, American Society of Mechanical Engineers2002*, pp. 487-96.
- [7] Y.K. Tan, *Energy harvesting autonomous sensor systems: design, analysis, and practical implementation*: CRC Press; 2013.
- [8] A. Harb, Energy harvesting: State-of-the-art, *Renewable Energy*, 36(2011) 2641-54.
- [9] S.P. Beeby, R. Torah, M. Tudor, P. Glynn-Jones, T. O'donnell, C. Saha, et al., A micro electromagnetic generator for vibration energy harvesting, *Journal of Micromechanics and microengineering*, 17(2007) 1257.
- [10] S. Chalasani, J.M. Conrad, A survey of energy harvesting sources for embedded systems, *Southeastcon, 2008 IEEE, IEEE2008*, pp. 442-7.
- [11] S. Roundy, On the effectiveness of vibration-based energy harvesting, *Journal of intelligent material systems and structures*, 16(2005) 809-23.
- [12] S.J. Roundy, *Energy scavenging for wireless sensor nodes with a focus on vibration to electricity conversion*: University of California, Berkeley Berkeley, CA; 2003.
- [13] S. Priya, D.J. Inman, *Energy harvesting technologies*: Springer; 2009.
- [14] C.A. Howells, Piezoelectric energy harvesting, *Energy Conversion and Management*, 50(2009) 1847-50.

- [15] H. Kim, Y. Tadesse, S. Priya, Piezoelectric energy harvesting, *Energy Harvesting Technologies*, Springer2009, pp. 3-39.
- [16] S. Saadon, O. Sidek, A review of vibration-based MEMS piezoelectric energy harvesters, *Energy Conversion and Management*, 52(2011) 500-4.
- [17] C.P. Le, E. Halvorsen, MEMS electrostatic energy harvesters with end-stop effects, *Journal of Micromechanics and Microengineering*, 22(2012) 074013.
- [18] E.O. Torres, G.A. Rincón-Mora, Electrostatic energy-harvesting and battery-charging CMOS system prototype, *IEEE Transactions on Circuits and Systems I: Regular Papers*, 56(2009) 1938-48.
- [19] F. Wang, O. Hansen, Electrostatic energy harvesting device with out-of-the-plane gap closing scheme, *Sensors and Actuators A: Physical*, 211(2014) 131-7.
- [20] S. Boisseau, G. Despesse, B.A. Seddik, Electrostatic conversion for vibration energy harvesting, arXiv preprint arXiv:12105191, (2012).
- [21] C.R. Saha, T. O'Donnell, H. Loder, S. Beeby, J. Tudor, Optimization of an electromagnetic energy harvesting device, *IEEE Transactions on Magnetics*, 42(2006) 3509-11.
- [22] B. Yang, C. Lee, W. Xiang, J. Xie, J.H. He, R.K. Kotlanka, et al., Electromagnetic energy harvesting from vibrations of multiple frequencies, *Journal of Micromechanics and Microengineering*, 19(2009) 035001.
- [23] R. Amirtharajah, A.P. Chandrakasan, Self-powered signal processing using vibration-based power generation, *IEEE journal of solid-state circuits*, 33(1998) 687-95.
- [24] N. Elvin, A. Erturk, *Advances in energy harvesting methods: Springer Science & Business Media*; 2013.
- [25] P. Miao, P. Mitcheson, A. Holmes, E. Yeatman, T. Green, B. Stark, MEMS inertial power generators for biomedical applications, *Microsystem Technologies*, 12(2006) 1079-83.
- [26] I. Kuehne, A. Frey, D. Marinkovic, G. Eckstein, H. Seidel, Power MEMS—A capacitive vibration-to-electrical energy converter with built-in voltage, *Sensors and Actuators A: Physical*, 142(2008) 263-9.
- [27] S. Meninger, J.O. Mur-Miranda, R. Amirtharajah, A. Chandrakasan, J.H. Lang, Vibration-to-electric energy conversion, *IEEE Transactions on Very Large Scale Integration (VLSI) Systems*, 9(2001) 64-76.
- [28] Y. Chiu, V.F. Tseng, A capacitive vibration-to-electricity energy converter with integrated mechanical switches, *Journal of Micromechanics and Microengineering*, 18(2008) 104004.

- [29] Z.J. Wong, J. Yan, K. Soga, A. Seshia, A multi-degree-of-freedom electrostatic MEMS power harvester, (2009).
- [30] D. Hoffmann, B. Folkmer, Y. Manoli, Fabrication, characterization and modelling of electrostatic micro-generators, *Journal of Micromechanics and Microengineering*, 19(2009) 094001.
- [31] G. Despesse, T. Jager, C. Jean-Jacques, J.-M. Léger, A. Vassilev, S. Basrour, et al., Fabrication and characterization of high damping electrostatic micro devices for vibration energy scavenging, *Proc Design, Test, Integration and Packaging of MEMS and MOEMS2005*, pp. 386-90.
- [32] Y. Zhang, T. Wang, A. Zhang, Z. Peng, D. Luo, R. Chen, et al., Electrostatic energy harvesting device with dual resonant structure for wideband random vibration sources at low frequency, *Review of Scientific Instruments*, 87(2016) 125001.
- [33] K. Tao, S.W. Lye, J. Miao, X. Hu, Design and implementation of an out-of-plane electrostatic vibration energy harvester with dual-charged electret plates, *Microelectronic Engineering*, 135(2015) 32-7.
- [34] M. Miyazaki, H. Tanaka, G. Ono, T. Nagano, N. Ohkubo, T. Kawahara, et al., Electric-energy generation using variable-capacitive resonator for power-free LSI: efficiency analysis and fundamental experiment, *Low Power Electronics and Design, 2003 ISLPED'03 Proceedings of the 2003 International Symposium on, IEEE2003*, pp. 193-8.
- [35] T. Sterken, K. Baert, C. Van Hoof, R. Puers, G. Borghs, P. Fiorini, Comparative modelling for vibration scavengers [MEMS energy scavengers], *Sensors, 2004 Proceedings of IEEE, IEEE2004*, pp. 1249-52.
- [36] F. Peano, T. Tambosso, Design and optimization of a MEMS electret-based capacitive energy scavenger, *Journal of Microelectromechanical Systems*, 14(2005) 429-35.
- [37] B.C. Yen, J.H. Lang, A variable-capacitance vibration-to-electric energy harvester, *IEEE Transactions on Circuits and Systems I: Regular Papers*, 53(2006) 288-95.
- [38] T. Tsutsumino, Y. Suzuki, N. Kasagi, Electromechanical modeling of micro electret generator for energy harvesting, *Solid-State Sensors, Actuators and Microsystems Conference, 2007 TRANSDUCERS 2007 International, IEEE2007*, pp. 863-6.
- [39] P. Basset, D. Galayko, A.M. Paracha, F. Marty, A. Dudka, T. Bourouina, A batch-fabricated and electret-free silicon electrostatic vibration energy harvester, *Journal of Micromechanics and Microengineering*, 19(2009) 115025.
- [40] P.D. Mitcheson, P. Miao, B.H. Stark, E. Yeatman, A. Holmes, T. Green, MEMS electrostatic micropower generator for low frequency operation, *Sensors and Actuators A: Physical*, 115(2004) 523-9.

- [41] D.-H. Choi, C.-H. Han, H.-D. Kim, J.-B. Yoon, Liquid-based electrostatic energy harvester with high sensitivity to human physical motion, *Smart Materials and Structures*, 20(2011) 125012.
- [42] P. Basset, D. Galayko, F. Cottone, R. Guillemet, E. Blokhina, F. Marty, et al., Electrostatic vibration energy harvester with combined effect of electrical nonlinearities and mechanical impact, *Journal of Micromechanics and Microengineering*, 24(2014) 035001.
- [43] V. Dorzhiev, A. Karami, P. Basset, F. Marty, V. Dragunov, D. Galayko, Electret-free micromachined silicon electrostatic vibration energy harvester with the Bennet's doubler as conditioning circuit, *IEEE Electron Device Letters*, 36(2015) 183-5.
- [44] K. Tao, J. Wu, L. Tang, L. Hu, S.W. Lye, J. Miao, Enhanced electrostatic vibrational energy harvesting using integrated opposite-charged electrets, *Journal of Micromechanics and Microengineering*, 27(2017) 044002.
- [45] P. Kotrappa, Long term stability of electrets used in electret ion chambers, *Journal of electrostatics*, 66(2008) 407-9.
- [46] Y. Chiu, Y.-C. Lee, Flat and robust out-of-plane vibrational electret energy harvester, *Journal of Micromechanics and Microengineering*, 23(2012) 015012.
- [47] Y. Sakane, Y. Suzuki, N. Kasagi, The development of a high-performance perfluorinated polymer electret and its application to micro power generation, *Journal of Micromechanics and Microengineering*, 18(2008) 104011.
- [48] H.-w. Lo, Y.-C. Tai, Parylene-based electret power generators, *Journal of Micromechanics and Microengineering*, 18(2008) 104006.
- [49] J. Boland, Y.-H. Chao, Y. Suzuki, Y. Tai, Micro electret power generator, *Micro Electro Mechanical Systems*, 2003 MEMS-03 Kyoto IEEE The Sixteenth Annual International Conference on, IEEE2003, pp. 538-41.
- [50] M. Soliman, E. Abdel-Rahman, E. El-Saadany, R. Mansour, A wideband vibration-based energy harvester, *Journal of Micromechanics and Microengineering*, 18(2008) 115021.
- [51] C.P. Le, E. Halvorsen, O. Søråsen, E.M. Yeatman, Wideband excitation of an electrostatic vibration energy harvester with power-extracting end-stops, *Smart Materials and Structures*, 22(2013) 075020.
- [52] D. Hoffmann, B. Folkmer, Y. Manoli, Fabrication and characterization of electrostatic micro-generators, *Proc PowerMEMS*, 15(2008).
- [53] P.D. Mitcheson, T. Sterken, C. He, M. Kiziroglou, E. Yeatman, R. Puers, Electrostatic microgenerators, *Measurement and Control*, 41(2008) 114-9.

- [54] V.R. Challa, M. Prasad, Y. Shi, F.T. Fisher, A vibration energy harvesting device with bidirectional resonance frequency tunability, *Smart Materials and Structures*, 17(2008) 015035.
- [55] M. Erismis, Design and modeling of a new robust multi-mass coupled-resonator family with dynamic motion amplification, *Microsystem technologies*, 19(2013) 1105-10.
- [56] C.W. Dyck, J.J. Allen, R.J. Huber, Parallel-plate electrostatic dual-mass resonator, *Micromachined Devices and Components V*, International Society for Optics and Photonics 1999, pp. 198-210.
- [57] K. Sahin, E. Sahin, S.E. Alper, T. Akin, A wide-bandwidth and high-sensitivity robust microgyroscope, *Journal of Micromechanics and Microengineering*, 19(2009) 074004.
- [58] K.-Y. Park, C.-W. Lee, Y.-S. Oh, Y.-H. Cho, Laterally oscillated and force-balanced micro vibratory rate gyroscope supported by fish-hook-shaped springs, *Sensors and Actuators A: Physical*, 64(1998) 69-76.
- [59] A. Shkel, R.T. Howe, R. Horowitz, Modeling and simulation of micromachined gyroscopes in the presence of imperfections, *Int Conf On Modelling and Simulation of Microsystems* 1999, pp. 605-8.
- [60] H. Xie, G.K. Fedder, Integrated microelectromechanical gyroscopes, *Journal of aerospace engineering*, 16(2003) 65-75.
- [61] R. Liu, H. Wang, X. Li, J. Tang, S. Mao, G. Ding, Analysis, simulation and fabrication of MEMS springs for a micro-tensile system, *Journal of Micromechanics and Microengineering*, 19(2008) 015027.
- [62] W.C. Young, R.G. Budynas, *Roark's formulas for stress and strain*: McGraw-Hill New York; 2002.
- [63] C. Acar, A.M. Shkel, Robust micromachined gyroscopes with two degrees of freedom sense-mode oscillator, *Google Patents* 2007.
- [64] S. Deevi, V. Sikka, Nickel and iron aluminides: an overview on properties, processing, and applications, *Intermetallics*, 4(1996) 357-75.
- [65] T.M. Pollock, S. Tin, Nickel-based superalloys for advanced turbine engines: chemistry, microstructure and properties, *Journal of propulsion and power*, 22(2006) 361-74.
- [66] Y. Suzuki, D. Miki, M. Edamoto, M. Honzumi, A MEMS electret generator with electrostatic levitation for vibration-driven energy-harvesting applications, *Journal of Micromechanics and Microengineering*, 20(2010) 104002.
- [67] Crovetto A, Wang F, Hansen O. An electret-based energy harvesting device with a wafer-level fabrication process. *J Micromech Microeng* 2013;23(October):114010.

- [68] Chiu Y, Lee YC. Flat and robust out-of-plane vibrational electret energy harvester. *J Micromech Microeng* 2013;24(December):015012.
- [69] Guillemet R, Basset P, Galayko D, Cottone F, Marty F, Bourouina T. Wideband MEMS electrostatic vibration energy harvesters based on gap-closing interdigitated combs with a trapezoidal cross section. In: 26th International conference on micro electro mechanical systems (MEMS), March 2013. p. 817–20.
- [70] Cottone F, Basset P, Guillemet R, Galayko D, Marty F, Bourouina T. Non-linear MEMS electrostatic kinetic energy harvester with a tunable multistable potential for stochastic vibrations. In: 17th International conference on solid-state sensors, actuators and microsystems (transducers & eurosensors XXVII), October 2013. p. 1336–9.
- [71] Minakawa Y, Chen R, Suzuki Y. X-shaped-spring enhanced MEMS electret generator for energy harvesting. In: 17th International conference on solid-state sensors, actuators and microsystems (transducers & eurosensors XXVII), October 2013. p. 2241–4.
- [72] DuPont™ Teflon® PTFE Specifications, [www.aetnoplastics.com](http://www.aetnoplastics.com)